DEMOCRATIC AND POPULAR ALGERIAN REPUBLIC

MINISTRY OF HIGHER EDUCATION AND SCIENTIFIC RESEARCH

SAAD DAHLEB BLIDA UNIVERSITY

Faculty of Sciences

Department of Physics

Dissertation for the completion of studies leading to the Master's degree in Physics

Specialization: Radiation Physics

Presented by

Chahih Samar and Benamar Lilia

Theme

Comparative study of the levels of essential and toxic elements in medicinal plants using the k_0-NAA technique

Jury :

President	Dr. R. Khelifi	Professor	USDB
Examiner	Dr. H. Slamene	Confirmed Researcher	CRNB
Supervisor	Dr. L. Hamidatou Alghem	Expert Researcher	CRND

June 2024

Acknowledgements

First of all, we thank God for guiding us to where we are now. We would like to thank the General Director of CRND for hosting us and contributing to the realization of this work. This work has been realized at the Nuclear Research Center of Draria (CRND) in Physics and Nuclear Application Division, Nuclear Techniques Department, Neutron Activation Analysis Laboratory.

We extend our deepest gratitude to our supervisor, Dr. Hamidatou Lylia Alghem, for her unwavering support, the valuable information she provided, and her constant encouragement throughout this project.

Special thanks to Mr. Guesmia Ahmed, Mr. Hadri Abderrazak, Mr. Khelili Rachid, Mr. Slamene Hocine, Dr. Samia Hadj Rabia for their significant help during the work process.

Our sincere appreciation goes to everyone in the Physics Department and the Matter Science Department who supported us in any capacity during our university career.

We would also like to warmly thank the members of the jury for accepting to review our work. Thank you for your time, expertise, and valuable feedback, which have greatly contributed to the improvement of our research.

Last but not least, our deepest thanks go to our parents and siblings, who have been with us since day one and have witnessed all our successes and failures. Thank you for your unwavering support, we hope we have made you proud today. Thank you all.

Dedication

To my parents, who have been there since day one, and have shown immense patience even when I wasn't always up to the task,
To my sisters, Habiba, Nawel, Sara, and Chaima, and my niece Sirine who have always believed in me, encouraged me in every way, and continue to do so,
To my grandmothers, whom I wish were still here to see what I have become today,
To myself, for not giving up, for always striving to improve, and for facing challenges head-on,
To my binome, Lilia, the best person I knew during my university studies,
To my laughter sharers, Ichrak, Anissa, Roufaida, Intissar,
To all Alkindi Club members,to everyone who encouraged me in one way or another,

This work is for you.
Samar Chahih

Dedication

I dedicate this work to my beloving parents , thank you for always being there through every step but gotta give extra love to my mom's car.

To my annoying siblings Fatma El Zohra and El Hacene i appreciate having you two there in bad and good times .

To my beautiful Grandmas , Grandpa , my amazing aunts on both sides , uncles and cousins , so grateful to have you as my familly .

Special love to my ml Partner Djihane , and to the sisters my mother never had Khadidja , Chaima , Miyada , Yassmine and Aisha can't be more happy to have you ladies in my life.

And the biggest appreciation goes to my handsome partner who made my university years one of the best Samar , we created the best memories along side Al kindi familly , best decision to join ever.

Lilia Benamar

Contents

List of Figures

List of Tables

List of Abbreviations

K0-NAA:	Kayzero Neutron Activation Analysis
PL:	Pistacia Lentiscus
LN:	Laurus Nobilis
RO:	Rosmarinus Officinalis
EE:	Essential Element
NEE:	Non Essential Element
INAA:	Instrumental Neutron Activation Analysis
WHO:	World Health Organization
CRM:	Certified Reference Material
SRM:	Standard Reference Material
C°:	Degree Celcius
HPGe:	Hyper Pure Germanium
KBq:	Kilo Becquerel
LEU:	Low Enriched Uranium
IAEA:	International Atomic Energy Agency
MCA:	Multi Channel Analyzer
ADC:	Analog to Digital Convertor
CRND:	Centre de Recherche Nucléaire Draria
COMENA:	Comissariat à l'Energie Atomique
PIPS:	Passivated Implanted Planar Silicon
SSB:	Surface Silicon Barrier
CdZnTe:	Cadmium Zinc Telluride
LaBr3:	Lanthanum Bromide
NaI(Tl):	Thallium-doped Sodium Iodide

Introduction

For millennia, medicinal plants have been a cornerstone of traditional medicine systems worldwide, celebrated for their therapeutic properties [1]. Notable examples include Laurel (Laurus nobilis), Pistacia (Pistacia lentiscus), and Rosemary (Rosmarinus officinalis), all of which are revered for their health benefits and widespread cultural use. These plants contain vital compounds beneficial to human health; however, they can also absorb toxic substances from their environment. Consequently, assessing the levels of these compounds is essential to guarantee the safety and therapeutic effectiveness of medicinal plants [2].

The central problem this work addresses is the lack of comprehensive data on the concentration of essential and toxic elements in these three medicinal plants. The scarcity of such data poses a challenge to ensuring the safe use of these plants in herbal medicine.

The efficient use of research reactors worldwide offers the possibility of providing research results in various fields [3].The NUR reactor in Algeria, a vital nuclear research facility, underscores the importance of nuclear infrastructure in advancing scientific research [4]. This 1 MW open pool reactor, operational since 1989 near Algiers, was integral to our study, providing a controlled environment for neutron activation analysis (NAA). This allowed us to conduct precise elemental analysis, crucial for our research [5]. The reactor's high neutron flux enabled the accurate and rapid determination of trace elements and heavy metals in samples studied, which was essential for the success of our experiments [6].

Various nuclear techniques, such as Neutron Activation Analysis (NAA) [1], Instrumental Neutron Activation Analysis (INAA) [7], X-ray Fluorescence (XRF) [8], Inductively Coupled Plasma Mass Spectrometry (ICP-MS), Prompt Gamma Neutron Activation Analysis (PG-NAA) [9], RadiochemicalNeutron Activation Analysis (RNAA) [10] are applied for elemental analysis. Among these, the k_0-NAA (k_0 Neutron Activation Analysis) technique stands out for its precision and reliability in detecting trace elements [11]. This method involves neutron irradiation of samples, resulting in the formation of radioactive isotopes. By measuring the

gamma radiation emitted from these isotopes, the elemental concentrations within the sample are determined. k_0 standardization based on neutron activation analysis is particularly advantageous due to its non-destructive nature and high sensitivity in identifying both major and trace elements [12].

By employing the k_0-NAA technique, this study aims to fill the data gap by providing precise and reliable measurements of essential and toxic elements in laurel, pistacia, and rosemary. This method is crucial for nutrient analysis, environmental monitoring, agricultural research, food safety, and plant physiology studies. It provides high sensitivity and precision, allowing for the detection of multiple elements simultaneously.However, it requires access to specialized facilities and careful handling of radioactive materials [4].

The overarching goal of this research is to analyze and compare the concentrations of essential and toxic elements in these medicinal plants using the k_0-NAA technique. This study seeks to contribute to the field of medicinal plant research by providing detailed elemental profiles of these plants [13].

Specifically, the research aims to determine the concentration levels of essential elements such as iron, zinc, and calcium in laurel, pistacia, and rosemary, quantify the presence of toxic elements such as arsenic, Vanadium, and Cromium in these plants, compare the elemental concentrations between the three plants and identify any significant differences or similarities, evaluate the safety of using these plants in medicinal preparations based on their elemental content.

This research is based on the hypothetico-deductive approach, operating under three main hypotheses: first, that laurel, pistacia, and rosemary contain varying concentrations of essential elements beneficial to health; second, that the levels of toxic elements in these plants are within safe limits for medicinal use; and third, that significant differences exist in the elemental composition of laurel, pistacia, and rosemary due to their differing growing environments and botanical characteristics.

The methodology involves the collection of plant samples from different regions, preparation and irradiation of samples using a neutron source, detection and analysis of gamma spectra to identify and quantify elements, and calibration of the detection chain for energy and efficiency to ensure accurate measurements .

This research contributes to the body of knowledge in the field of medicinal plant studies by providing detailed elemental profiles of laurel, pistacia, and rosemary. It offers a scientific basis for understanding the nutritional and toxicological properties of these plants, which is essential for their safe use in herbal medicine. The findings of this study have significant practical implications. They can be used to inform regulations and guidelines for the safe use of medicinal plants. Additionally, this research can aid in the development of quality control standards for herbal products, ensuring that they are safe for consumer use [14].

This work is structured as follows: Chapter 1 covers generalities, providing an overview of laurel, pistacia, and rosemary, and the k_0-NAA technique. Chapter 2 delves into detection, gamma spectroscopy, and calibration, detailing the detection process and calibration methods. Chapter 3 describes the experimental part, including a comprehensive description of the materials, methods, irradiation process, validation of results, and discussion. This structured approach ensures a thorough exploration of the elemental composition of the selected medicinal plants and provides a solid foundation for the conclusions and recommendations drawn from the research.

Chapter 1

Generalities

In this chapter, we are going to embark on a multifaceted exploration of three distinct medicinal plants Pistacia Lentiscus, Laurus nobilis, and Rosemarinus officinalis. The first segment will delve into an in-depth bibliographical research, shedding light on the historical, ecological, and medicinal aspects of these botanical subjects. This thorough investigation will establish a solid foundation for the subsequent sections. The chapter will seamlessly transition into the second part, dedicated to elucidating the technique employed in the study, the k_0 standardization based on neutron activation analysis (k_0-NAA) method, this portion will expound on the procedural intricacies and underlying principles that form the backbone of our research methodology. Together, these two facets will provide a holistic introduction to the scope and methodology of the study, laying the groundwork for the subsequent chapters of the project.

1.1 Pistacia Lentiscus

1.1.1 Generalities

Pistacia lentiscus, commonly referred to as the mastic tree or lentisk or just Pistacia, is a dioecious, wild, ecologically responsible, evergreen shrub, three meters in height, belonging to the Anacardiaceae family, Sapindales Order, bearing vibrant red spherical berries. It thrives in challenging growing conditions, warm regions at low altitudes and in sunny, sheltered areas at medium altitudes (<1,100m above sea level) [15–18].
it has the capacity to withstand and accumulate salt, likely contributing to its prevalence in Mediterranean coastal areas.including dryness and warm climates, all of which impact its genotype and the abundance of secondary metabolites. It belongs to a diverse family of eleven species. It is pollinated by wind. In this species, male and female flowers occur on separate trees. Flowering takes place from mid-March to late April. Male inflorescences consist of 8-10

clustered flowers. Female flowers bear a single seminal primordium. Male tree flowers are deep red, while female tree flowers are yellow.The leaves are alternately arranged, thick and shiny, dark green, with a strongly acrid resin odor, organized in compound, pinnate whorls. Unisexual flowers are clustered together. The round fruit is a fleshy drupe [16, 18–20].
PL is susceptible to developing leaf galls due to insect infestation, notably from aphids. Various classifications have been proposed for the Pistacia genus, with one of the most renowned being that of Zohary. Zohary's classification divides the genus into four main groups based on leaf and nut morphology characteristics. The essential oil extracted from the gum/resin is commonly known as mastic oil, while the oil obtained from the leaves is referred to as lentisk oil [16, 18].

Figure 1.1: Pistacia lentiscus L. plant [16]

1.1.2 Distribution

PL is found globally within a region spanning from the twentieth to the forty-fifth north parallel. Its trees are notable components of the flora in the Mediterranean basin and Middle East. Its range across the Mediterranean basin also encompasses North and Eastern Africa, as well as Madeira Island. It is among the most common shrubs found in the maquis (shrubland) ecosystems of Europe, Morocco, Turkey, Iraq, and Iran. In Italy, it is a distinctive feature of sensitive ecosystems such as Sardinia, where it thrives along the coast up to 700 meters above sea level. This plant is particularly representative of the warmest environments in the Mediterranean climate [16, 19, 21–23].

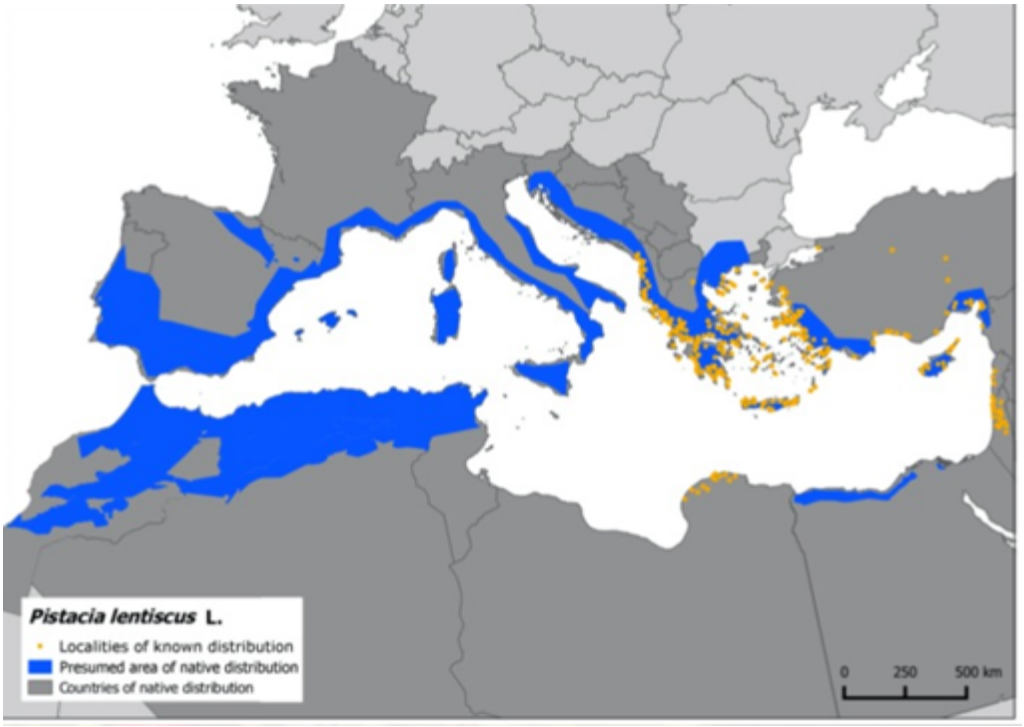

Figure 1.2: Distribution of Pistacia lentiscus L. in the world [24]

1.1.3 Chemical Composition

PL contains various medically significant compounds like resin, essential oils, gallic acid, anthocyanins, flavonol glycosides, triterpenoids, tocopherol, and arabinogalactan proteins. Its leaf, stem, fruit, and root are rich in bioactive phenolic compounds. Lentisk extracts are abundant in polyphenols, flavonoids, tannins, and proanthocyanidins, with yield depending on the extract type and plant part used [15].

1.1.3.1 Physico-chemical Properties of Essential Oil

Research on PL resin and essential oils across the Mediterranean reveals diverse compositions. In Spain, resin is dominated by α-pinene and myrcene, while Corsican leaf oil is rich in $tepinen-4-ol$ and α-pinene. Greek mastic gum oil primarily comprises α-pinene ($58.9-70\%$), contrasting with Egyptian varieties featuring car-3-ene as a major component (65%). These oils are characterized by terpenes and terpenoids, notably monoterpenes and sesquiterpenes, influenced by genetics, growing conditions, and harvest times. P. lentiscus essential oil contains up to 64 chemical constituents, including α-pinene, myrcene, limonene, (E)-β-caryophyllene, and γ-terpinene, each with pharmacological properties potentially beneficial in immune-related and neurological conditions [17, 18, 21, 25].

1.1.4 Pharmacological Effects

The medicinal plant PL exhibits notable pharmacological characteristics, including antioxidative, antimicrobial, anticancer, anti-inflammatory, antibacterial, and antifungal effects, making it promising for therapeutic use. Its phenolic extracts demonstrate significant antioxidant capacity through various assays, attributed to their elevated phenolic compound levels. In vitro studies highlight its anticancer potential against several cancer cell types, supported by its flavonoid and phenolic compound content. P. lentiscus also shows anti-inflammatory effects in animal models, with its essential oil containing anti-inflammatory terpenes inhibiting inflammatory molecules. Ongoing research explores its antibacterial effects, with mastic oil and its components exhibiting potency against pathogenic bacteria. Additionally, its aqueous leaf extract demonstrates strong antifungal activity against dermatophytes, suggesting its potential in treating fungal infections [15, 16, 18].

1.2 Laurus Nobilis

1.2.1 Generalities

Laurus nobilis L.,The first part of the scientific name, Laurus, originates directly from the Latin term for the tree, likely derived from an older Celtic term, blaur, signifying green. Meanwhile, nobilis, also from Latin, signifies noble and renowned.LN has been revered since ancient times, being dedicated to Apollo, the ancient Greek deity associated with light. It symbolizes peace and victory, often fashioned into wreaths for emperors, generals, and poets. commonly known as Grecian laurel,bay laurel, sweet bay, laurel, true bay, or simply bay. This fragrant tree typically ranges in height from 2 meters to 10 meters, Nevertheless, in garden and yard settings, the typical dimensions are generally smaller, ranging from 4 to 6 meters. Its leaves are arranged alternately, being narrowly oblong-lanceolate in shape, it measure 5-8 cm in length and 3-4 cm in width, featuring a glossy olive-green to brown upper surface and a matte olive to brown underside with prominent veins. When crushed, they release a fragrant aroma and have a bitter, aromatic flavor. Its small yellow-white flowers blossom in spring (March-May), giving way to berry-like fruits with a single seed. Initially green, these berries ripen into vivid bluish-black fruits. Dried fruits are oval-shaped, approximately 15 mm long and 10 mm wide [26–30].

Figure 1.3: Laurus Nobilis L.plant [16]

1.2.2 Distribution

Laurel typically thrives in sunny locations within regions characterized by warm climates and abundant rainfall. This plant is prevalent in North African countries such as Tunisia, Algeria, and Morocco,and Mediterranean countries such as Turkey, Spain, Italy, Greece, and Portugal. It can also be found in tropical and subtropical regions of Asia, Australia, the Pacific, and South Asia. Turkey, Italy, Belgium, Algeria, France, Tunisia, Iran, Morocco, Serbia, Greece, Portugal, Central America, and the Southern United States serve as major commercial hubs for bay leaf production [26, 31, 32].

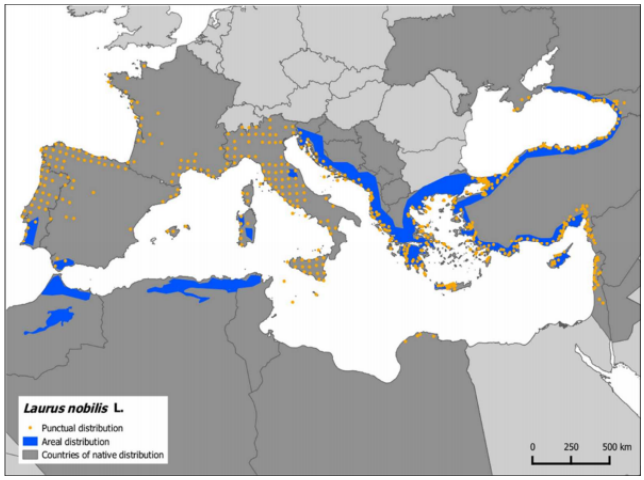

Figure 1.4: Distribution of L. Nobilis [26]

1.2.3 Chemical Composition

Extensive research has been conducted on the chemical composition of LN, The significant commercial and medicinal value of this plant stems from its important chemical composition [28, 31].

The chemical composition of Laurus nobilis dried leaves includes moisture at 4.5%, protein at 7.6%, fat at 8.8%, fiber at 25.2%, carbohydrates at 50.2%, and total ash at 3.7%. Additionally, it contains calcium at 1%, phosphorus at 0.11%, sodium at 0.02%, and potassium at 0.6%. Iron is present at 0.53%. In terms of vitamins per 100g, it contains Vitamin B1 at 0.1%, Vitamin B2 at 0.42%, niacin at 2.0%, Vitamin C at 46.6%, and Vitamin A at 545 IU. Its calorific value is 410 calories per 100g.

The analysis of Laurus nobilis leaves reveals a composition consisting of 9.45% moisture, 8.34% protein, 4.49% fixed oil, 3.63% volatile oil, 25.01% alcohol extract, 38.33% nitrogen-free extract, 31.83% fiber, 4.53% ash (Italian variety), and 13.84% pentosans [33].

1.2.3.1 Physico-chemical Properties of Volatile Oil

According to Parry (1969), laurel leaves produce volatile oil at a rate of 1–3%, with specific gravity at 15 °C ranging from 0.915 to 0.930 and optical rotation at 20 °C between 15 and 22 degrees Celsius. The refractive index at the same temperature falls within 1.4670 to 1.4775. The main constituent, cineol, comprises 25% to 50% of the total composition and is soluble at a ratio of 1 part to 3 parts of 80% alcohol. Additionally, laurel oil contains various organic compounds such as α-pinene, α-phellandrene, 1-linalool, 1-β-terpineol, geraniol, eugenol, eugenol acetate, methyl eugenol, along with several esters, and acids including acetic, isobutyric, and isovaleric acids [33].

1.2.4 Pharmacological Effects

Extensive research has been conducted on the biological activities and phytochemistry of LN in the past. In recent studies, pharmacological activities such as antibacterial, antifungal, antidiabetic, antioxidative, and anti-inflammatory effects, as well as insecticidal properties, have been observed. These activities have traditionally been linked to the essential oil components of the substances [31, 32].

The lyophilized aqueous and ethanol extracts of LN displayed potent antioxidant properties, while the seed extracts showed antiulcerogenic effects in a rat model. LN leaf essential oil exhibited anticonvulsant activity but induced sedation at higher doses. It also had analgesic and anti-inflammatory effects comparable to morphine and piroxicam, with neuroprotective effects against dopamine-induced cell damage and Parkinson's disease models. L. nobilis ex-

tract yielded a purified antimutagen, and essential oils showed antiviral and insect repellent activity. The methanolic extract exhibited superior antibacterial activity, while the leaf oils displayed acaricidal activity against Psoroptes cuniculi [30].

1.3 Rosemarinus Officinalis

1.3.1 Generalities

Rosemary (R. officinalis L.), a member of the Lamiaceae family originating from the Mediterranean. Its fragrant green leaves make it a versatile plant, serving as a spice in cooking, a natural preservative in the food industry, and an ornamental and medicinal plant. Rosmarinus officinalis is a perennial shrub celebrated for its aromatic and woody qualities, making it a prized plant across various domains. With an upright growth habit, this evergreen herb forms a robust bush with multiple branches, attaining a maximum height of 2 meters. The leaves, reminiscent of pine needles, measure approximately 2-4 centimeters in length and 2-5 millimeters in width, showcasing a vivid green color on the upper side and a contrasting white tone beneath []. Notably, the leaves boast a dense covering of short woolly hairs. A defining feature of RO lies in its distinctive fragrance, derived from the aromatic oils found within the leaves. This aromatic quality has propelled the plant's popularity in both culinary and medicinal applications. In-depth descriptions of RO's botanical characteristics can be found in scientific articles such as "Chemical composition of Rosmarinus officinalis L. essential oil and its antibacterial activities against foodborne pathogens [34–36].

Figure 1.5: Rosemary plant [37]

1.3.2 Distribution

Rosemary, originating from the western Mediterranean basin, boasts diverse genetic diversity. Cultivated since ancient times, it serves various purposes, including ornamental landscaping, pot cultivation, and the production of leaves and essential oil. Studies suggest multiple migration routes, including northern, southern via North Africa to Cyrenaica, and southwest from the Iberian Peninsula, influencing its demographic expansion [35].

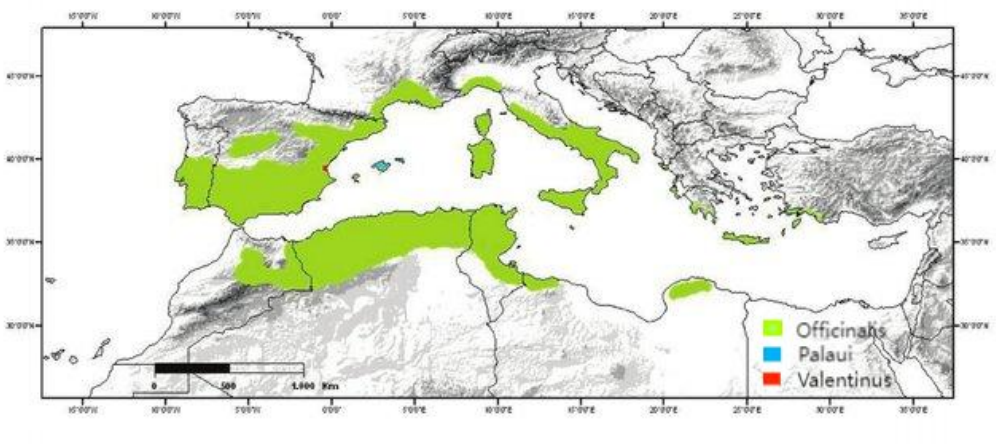

Figure 1.6: Distribution of Rosemary plant in the world [38]

1.3.3 Chemical Composition

In various regions, studies have identified different major constituents in RO. These include α-pinene, camphor, 1,8-cineole, camphene, α-terpineol, and borneol in Greece. In China, predominant components were 1,8-cineole, α-pinene, camphor, camphene, and β-pinene. Italian research highlighted α-pinene and 1,8-cineole. In Brazil, α-pinene and camphene were primary components. Spanish studies noted α-pinene, 1,8-cineole, and camphor. Ethiopian studies reported common compounds such as 1,8-cineole, verbenone, camphor, α-terpineol, isoborneol, tridecyl acrylate, linalool, bornyl acetate, trans-caryophyllene, terpinen-4-ol, and α-pinene [36, 39–41].

1.3.4 Pharmacological Effects

Rosemary displays various pharmacological effects supported by research: rosmarinic acid and carnosol provide anti-inflammatory benefits, while its antioxidant content, including flavonoids and diterpenes, neutralizes free radicals. Studies suggest neuroprotective properties, benefiting cognitive function and protecting against neurodegenerative disorders. Rosemary extracts exhibit antimicrobial and antibacterial effects and show promise as anticancer agents, inhibiting

cancer cell growth and inducing apoptosis [36, 39, 41].
Traditionally used for digestive issues, rosemary's antispasmodic properties may alleviate intestinal spasms. Additionally, rosemary contributes to cardiovascular health by improving circulation, reducing oxidative stress, and potentially lowering blood pressure, while research suggests its anti-diabetic effects in regulating blood sugar levels [40, 42, 43].

1.3.5 Uses of Laurel, Pistacia, and Rosemary

RO, LN, and PL have been used since eternity in various fields beyond medicine, including cosmetics, culinary arts, and more. These versatile plants have found applications in enhancing beauty, flavoring dishes, and providing aromatic experiences, making them indispensable in everyday life. The table 1.1 summarizes the uses of these three plants across different domains.

Table 1.1: Uses of the three plants

Uses	**Pistacia**	**Laurel**	**Rosemary**
Medicinal uses	phyto stabilizer [16], gastrointestinal issues, eczema and throat infections, oral infections, diarrhea, kidney stones, jaundice, headaches, asthma, and respiratory issues [21]	antimicrobial, cytotoxic, and immune-modulating activities [29], managing cardiovascular diseases and addressing low blood pressure [44]	anti-inflammatory and antioxidant properties, aiding digestion, and cognitive functions [36]
Culinary uses	flavoring agent in liqueurs and jams, breath-freshening chewing gum [21]	seasoning meat products, soups, fish [30], stews, puddings, vinegar and beverages [26], broths and vegetables [44]	enhances the flavor of dishes like meats, stews, soups, and roasted vegetables [35]
Cosmetic uses	nourishes, protects, and moisturizes the skin, softens damaged skin [45]	the production of soap [30], production of creams, perfumes [27]	skincare and hair care products for their antimicrobial qualities [39]

1.4 k_0-NAA technique

1.4.1 Background

Neutron activation analysis (NAA) is a technique used for assessing the mass fractions of chemical elements by initiating radioactivity through neutron irradiation and subsequently detecting the emitted radiation.
For accurate results, neutron activation analysis requires standardization. The single- comparator method simplifies the process by relating the sensitivity of all elements to a chosen one. Co-irradiating and measuring standards of the comparator element with the unknown sample streamlines the procedure. Increased flexibility is achieved by determining detector efficiency separately for various counting geometries. The resulting "k factors," akin to compound nuclear constants, only need determination once for each irradiation facility. Further flexibility is attained through neutron spectrum modeling, requiring characterization via a few parameters. The initial "k factor" is later termed " k_0 factor," introduced in 1975, and quickly gains global recognition for its simplicity and effectiveness in instrumental neutron activation analysis (INAA) [46–48].

1.4.2 *Hϕgdhal* Convention and Westcott Formalism

The Hogdhal conversion and the Westcott formalism are two methods used in neutron activation analysis to describe neutron capture cross-sections. The Westcott formalism, developed by Charles Westcott in the 1950s, is a widely used approach that defines the effective cross-section of a nuclide by taking into account the Maxwellian distribution of neutron velocities at a thermal energy of 0.0253 eV (25.3 meV) at room temperature. This method is effective for reactors where thermal neutrons play a significant role and incorporates factors like the Westcott g-factor and resonance integrals. In contrast, the Hogdal conversion, introduced by Norwegian physicist Olav Hogdal in the 1960s, is a more generalized approach that can account for a broader range of neutron energies, including epithermal neutrons, by integrating the neutron flux and cross-section over all relevant energies. This conversion is particularly useful for systems with significant contributions from both thermal and epithermal neutrons. While the Westcott formalism remains prevalent in many standard applications, the Hogdal conversion provides a more comprehensive framework for environments where the neutron energy spectrum is more complex [49].

1.4.3 Fundamental Formula

Acording to the Hogdhal conversion, in the first sets of expressions used by Simonits , the linear relation between the count rate in a specific gamma ray peak and the amount of element present in the sample was expressed with [50] :

$$N_p/t_m = w\left(\frac{\gamma\theta N_a}{M}\right)(\phi_s\sigma_0 + \phi_{epi}I_0)SDC\epsilon \tag{1.1}$$

Np peak area,
t_m measurement time (s),
w weight of element (g),
γ gamma ray yield,
θ isotopic abundance
N_a Avogadro's number,
M atomic mass (g),
ϕ_s subcadmium (a.k.a. thermal) neutron fluence rate ($m^{-2}s^{-1}$),
σ_0 thermal capture cross section (m^2),
ϕ_{epi} epicadmium (a.k.a. epithermal) neutron fluence rate ($m^{-2}s^{-1}$),
I_0 resonance integral (m^2)
S saturation factor,
D decay factor,
C counting factor,
ϵ detection efficiency.
Here, the saturation factor S is defined as :

$$S = (1 - e^{-\lambda t_{irr}}) \tag{1.2}$$

λ is the decay constant (s^{-1}) and t_{irr} is the irradiation time (s).
The decay factor D is defined by :

$$D = e^{-\lambda t_d} \tag{1.3}$$

t_d is the decay time between irradiation time and measurement (s).
The counting factor C is defined by :

$$C = \frac{(1 - e^{-\lambda t_m})}{\lambda t_m} \tag{1.4}$$

where t_m is the duration of the measurement (s)
S, D and C can get more complicated if the radionucleid measured in the end is not exclusively

and directly produced by a single (n,γ) reaction. With the definition of $Q_0 = I_0/\sigma_0$, the main expression becomes :

$$N_p/t_m = w\left(\frac{\gamma\theta N_a}{M}\right)(\phi_s + \phi_{epi}Q_0)SDC\epsilon \tag{1.5}$$

1.4.4 Non-ideal Epithermal Neutron Spectrum, Self-Shielding and True Coincidence Summing

To account for the non-ideal epicadmium neutron spectrum shape, an α -parameter was introduced to quantify the deviation. The effective resonance energy (E_r) was also incorporated to represent the reaction's sensitivity to α. Consequently, both the resonance integral (I_0) and Q_0 became functions of α. The relationship between $Q_0(\alpha)$, α, and the effective resonance energy E_r is expressed as follows [50]:

$$Q_0(\alpha) = \frac{Q_0(0) - 0.429}{E_r^{\alpha}} + \frac{0.429}{(2\alpha+1)E_{C_d}^{\alpha}} \tag{1.6}$$

Where :

E_{C_d} is the C_d-cutoff energy (0.55 eV),

E_r is the effective resonance energy (eV).

Correction factors (g_{th} and g_{epi}) handle neutron self-shielding during irradiation, while a factor (c) corrects for true coincidence summing during measurement. Detector efficiency (ϵ) accommodates variations in counting geometry due to sample distance, shape, and gamma ray self-absorption.

$$N_p/t_m = w\left(\frac{\gamma\theta N_a}{M}\right)(g_{th}\phi_s\sigma_0 + g_{epi}\phi_{epi}I_0(\alpha))SDC\epsilon \tag{1.7}$$

$I_0(\alpha)$ is the α-dependent resonance integral (m^2),

α the parameter that accounts for non-ideal 1/E epicadmium flux distributions,

g_{th} the thermal self-shielding factor,

g_{epi} the epithermal self-shielding factor,

and C is coincidence correction factor.

With the reaction rate being given as [51] :

$$R = K\int_0^{\infty}\sigma(E)\phi(E) \tag{1.8}$$

Without loss of generality, the expression commonly used in NAA for reaction rates is given by [51]:

$$R = \phi_t\sigma_0 gG_t + \phi_f IG_f = \phi_t\sigma_0[gG_t + \frac{1}{f}QG_f] \tag{1.9}$$

where the symbols have the following meaning:
ϕ_t thermal flux,
ϕ_f epithermal flux,
f ratio of thermal to epithermal flux $\frac{\phi_t}{\phi_f}$,
σ_0 thermal cross section at 2200 m/s neutron speed, g generalised g-factor that measured the deviation of the thermal cross section from 1/v shape,
I effective resonance integral,
Q ratio of the resonance integral and the thermal cross section $\frac{I}{Q_0}$,
G_t thermal flux depression factor,
G_f resonance self-shielding factor.
In NAA's k_0 standardization method, activities are compared to a well-defined standard, typically gold. Gold is chosen for its known cross sections and easily measurable gamma ray intensity. The ratio of sample activity (A_a) to standard activity (A_s) is linked to the ratio of reaction rates, expressed as [50]:

$$\frac{A_a}{A_s} = K_0, a\frac{G_t f g_a + G_f, aQ_a}{G_t f g_s + G_f, sQ_s} \tag{1.10}$$

With the definition of the k_0 [52] :

$$k_{0,a} = \frac{(\frac{\sigma_{0,c}\gamma_a\theta_a}{M_a})}{(\frac{\sigma_{0,Au}\gamma_{0,Au}\theta_{Au}}{M_{Au}})} \tag{1.11}$$

How the factor is calculated :

$$k_0, a = \frac{(N_p/wt_m SDC)a}{(N_p/wt_m SDC)Au}\frac{f + Q_{0,Au}(\alpha)}{f + Q_{0,a}(\alpha)}\frac{\epsilon_{p,Au}}{\epsilon_{p,a}} \tag{1.12}$$

Therefore, we have settled to use the equation (1.12) in the experimental part of our work.

1.4.5 Application of the k_0-NAA Technique

NAA is particularly useful for the quantitative analysis of trace elements in rock samples, making it a valuable tool for modeling geochemical processes and aiding in sample selection for various applications. Additionally, this method is employed in the production of radiotracers, which are used in situ to evaluate new pharmaceuticals in terms of their distribution, time release, clearance, and more.
The k_0-Neutron Activation Analysis (k_0-NAA) technique serves diverse applications. It's vital in Environmental Science for pinpointing pollutants, aids Material Science in characterizing materials, advances Nuclear Reactor Studies by studying neutron flux,

and facilitates Biomedical Research in disease diagnosis. It can also be beneficial in treating certain conditions, such as Alzheimer's disease In Industry, it ensures product integrity through accurate elemental analysis, while in Research Laboratories, its sensitivity drives innovations across disciplines [53–61].

Chapter 2

Detection and Calibration

This chapter introduces the principles of alpha, beta, and gamma spectroscopy, focusing on the detection and analysis of each type of radiation. It also covers energy and efficiency calibration techniques crucial for accurate measurements, along with addressing the summing effect phenomenon in spectroscopic analysis.

2.1 Alpha, Beta, Gamma Spectroscopy

2.1.1 Alpha Spectroscopy

Alpha spectroscopy stands as a widely employed method for discerning and measuring alpha-emitting radionuclides, encompassing both naturally occurring alpha emitters and transuranic elements including special nuclear materials. Renowned for its high efficiency, minimal background noise, and impressive detection thresholds, this technique finds application across diverse sample types. Notably, the laboratory alpha spectrometry system predominantly utilizes silicon semiconductor detectors such as PIPS and SSB, with careful consideration given to the selection of collection media. Glass fiber filters, chosen for their superior "front surface" collection attributes, are favored in alpha spectrometers to prevent the entrapment of collected particles within the filter bed [62].

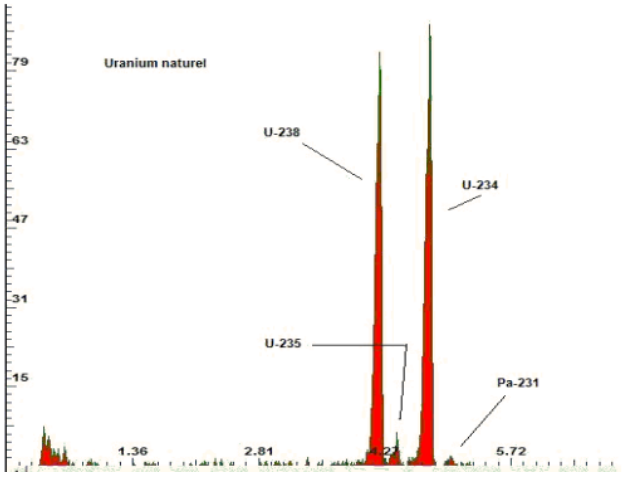

Figure 2.1: Alpha spectrum recorded using surface barrier detectors [62]

The spectrum showing in Figure 2.1 depicts the alpha spectrum of natural uranium, recorded using surface barrier detectors. It features distinct peaks for U-238, U-234, and U-235, as well as Pa-231. The x-axis represents the energy of alpha particles in MeV, while the y-axis shows the intensity, indicating the number of particles detected at each energy level. The clear separation and height of these peaks provide valuable information on the isotopic composition and decay processes in natural uranium.

2.1.2 Beta Spectroscopy

Unlike alpha/gamma spectrometry, pure beta emitters exhibit continuous spectra. Existing literature primarily addresses methods for spectral beta total and gamma discrimination for dosimetry purposes. Electrons can be distinguished based on various characteristics, including their spectral shape, maximum beta energy of the transition, and the presence of gamma-emitting nuclides, where conversion electron peaks (e.g., Cs-137, Co-60) may also be utilized [63].

2.1.3 Gamma Spectroscopy

For Gamma spectroscopy, it relies on three fundamental interactions of radiation with matter: the photoelectric effect, Compton scattering, and pair production, with interaction probability influenced by atomic number, material density, and gamma ray energy. Various detector types are employed, including NaI(Tl) for high efficiency and HPGe for superior resolution, with setup involving calibration using reference sources. Different spectrometer types like NaI(Tl), HPGe, CdZnTe, and LaBr3 are chosen based on efficiency, resolution, and cooling requirements. This analytical tool enables the identification and quantification of gamma-emitting

isotopes in diverse samples, involving peak identification, energy determination, radionuclide identification, peak area calculation, background subtraction, and activity determination, often supported by spectrometry software for efficient analysis [62].

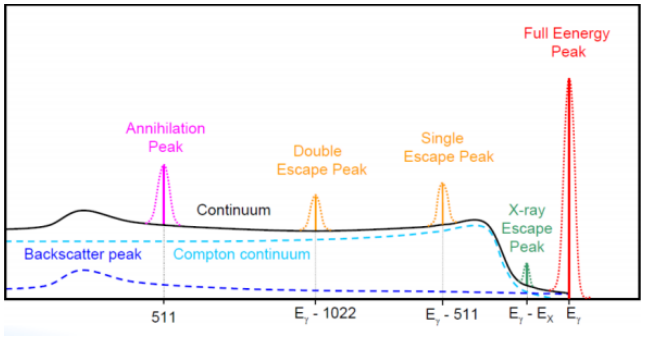

Figure 2.2: Theoretical spectrum of gamma ray [62]

Gamma ray spectrometry has diverse applications, including analyzing lab samples with HPGe systems and using portable HPGe for contamination monitoring, especially surface contamination in workplaces. These systems aid in qualitatively identifying contaminants and radionuclides. They're also useful for identifying unknown isotopes in containers. Various portable gamma spectrometric systems are available for qualitative analysis, albeit with limited energy resolution, primarily detecting distinct radionuclides.
Additionally, different systems are compared for in-situ monitoring tasks. Lastly, gamma spectrometry is vital for air monitoring applications [62].

2.2 Constitutions of Spectrometry Chain

In general, all elements that compose a gamma spectrometry chain must have the property of linearity, meaning there is proportionality between the energy absorbed and the resulting final pulse. The classic measurement chain consists of a detector (Figure 2.4), preamplifier (Generation of a pulse with amplitude directly correlated to the energy absorbed by the detector) , amplifier (signal shaping), analog-to-digital converter (ADC; conversion of the analogue signal into digital value), acquisition electronics (recording of the events received on a memory), and analysis software (piloting of the spectrum acquisition, visualisation and processing). The following figure represents the diagram of a measurement chain dedicated to gamma spectrometry [62, 64]. The Figure (2.4) represents a semi conductor detector used generally in gamma spectroscopy.

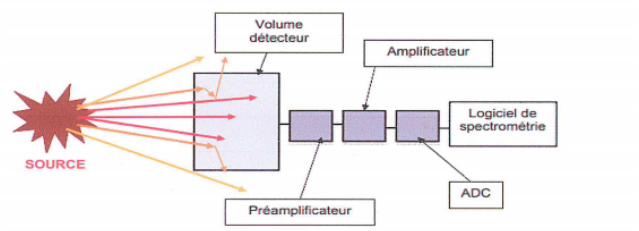

Figure 2.3: Measurement chain dedicated to gamma spectrometry [64]

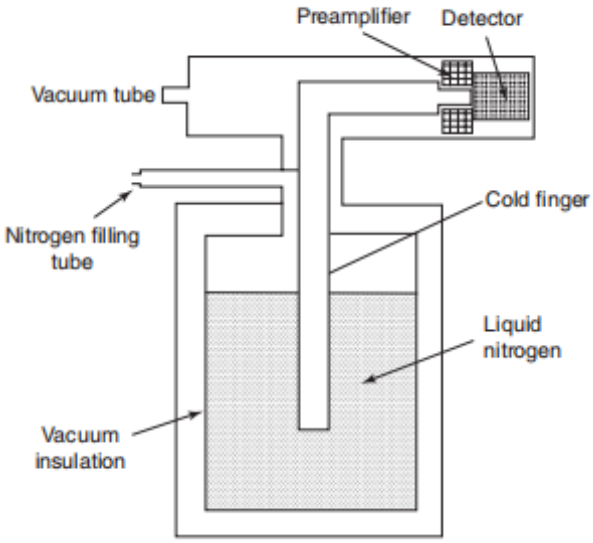

Figure 2.4: Schematic cross-sectional view of a semiconductor detector for gamma-ray spectrometry with liquid nitrogen Dewar [65]

2.3 Spectrometry Chain Calibration

The gamma spectrometry chain calibration involves two main stages: energy calibration, which ensures detector linearity and identifies radionuclides in the sample, and efficiency calibration, used to determine radionuclide activity.

2.3.1 Energy Calibration

Prior to any measurements, the initial step involves calibrating the energy within the gamma spectrometry chain to ensure precise identification of radioelements in samples. Energy calibration entails associating energy levels with the channels of the MCA, establishing a correlation between energy and channel number. To achieve this, a point radioactive source with known gamma energies was utilized [66].

We employed Europium (Eu-152) as the radiation source. The activity of the source was measured at 386.3 (KBq), and it was fabricated on July 1st, 1985. With a half-life of 13.6 years, the Eu source provided stable and reliable radiation emissions for calibration purposes. To ensure accurate measurements, we positioned a geometry between the source and the detector (HPGe, 30%), maintaining a distance of 11 centimeters. Subsequently, we obtained a spectrum for energy calibration, conducting the measurement over a period of 315 seconds. This calibration process allowed us to establish a precise correlation between energy levels and channel numbers in the spectrometer. After the energy calibration, we condensed the energy values and their corresponding channel numbers into the table below.
This table simplifies the process of identifying energy levels during spectroscopic analysis.

Table 2.1: Values of Eu-152 gamma rays related to their channels

Energy (Kev)	**Channel**	**Energy (Kev)**	**Channel**
121.78	243.56	778.89	1557.78
244.69	489.38	964.01	1928.02
344.27	688.54	1112.02	2224.04
411.11	822.22	1407.95	2815.9
443.97	887.94		

The calibration energy straight line is presented in the Figure 2.5 :

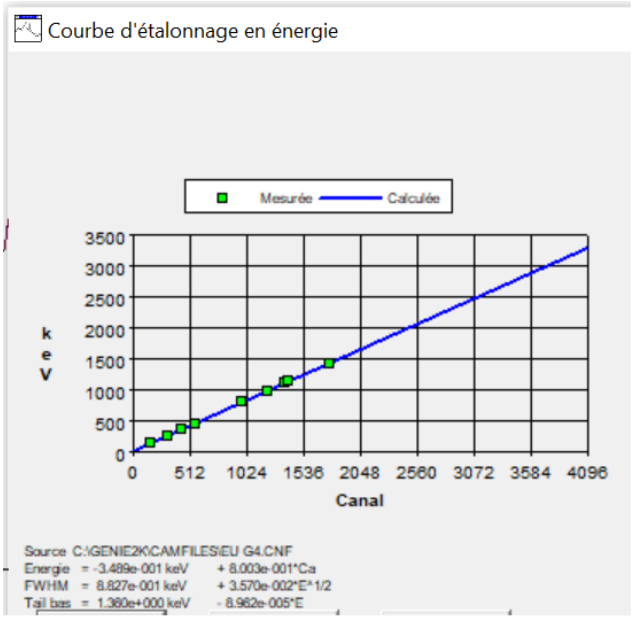

Figure 2.5: Calibration line of Eu-152 source obtained with Genie 2k [67]

2.3.2 Efficiency Calibration

The crucial step in gamma-ray spectrometry is quantifying the photons emitted by a source and detected by the detector. Detector efficiency is essential for accurate gamma radiation measurement. The efficiency of a detector system is heavily influenced by factors like gamma-ray energy, detector and source dimensions, geometric setup, and sample density. As a result, calibration for one detector may not apply to another [68].
Five standard gamma point sources (Barium-133,Cesium-137, Cobalt-60, Europium-152, and Americium-242) were used to characterize the gamma ray spectrometer with an HPGe detector at the Draria Nuclear research center, at various source–detector distances.

Table 2.2: Data of gamma source

Source	**Date of fabrication**	A_0**(KBq)**	A**(kBq)**	$T_{1/2}$ **(days)**
Am-241	01-07-1985	364.0	342.075	157850
Ba-133	01-07-1985	299.8	23.561	3848
Co-60	01-07-1985	460.2	2.910	1925.2
Cs-137	01-07-1985	378.7	155.040	11031.23
Eu-152	01-07-1985	386.3	52.917	4941

The efficiency ϵ of the detector is then calculated using the formula [69] :

$$\epsilon = \frac{N}{AI_\gamma t_m} \tag{2.1}$$

Where :
N is the number of counts per second within the full-energy peak
A is the activity of the gamma-ray source
I_γ is the gamma-ray emission intensity
t_m is the measurement time
The activity of gamma ray source is calculated using the formula [66] :

$$A = A_0 e^{-\frac{Ln2t_d}{T1/2}} \tag{2.2}$$

Where :

A_0 is the initial activity of the source

$T_{1/2}$ is the period of the source

The efficiency measurement error is determined using the error propagation law, which is influenced by the uncertainties associated with parameters such as the total absorption peak surface area (N), gamma intensity (activity outside the source), and counting time. The uncertainty in detector efficiency measurement is expressed by the following relationship [66]:

$$\frac{\delta\epsilon}{\epsilon} = \left[\left(\frac{\delta N}{N}\right)^2 + \left(\frac{\delta A}{A}\right)^2 + \left(\frac{\delta\gamma}{\gamma}\right)^2 + \left(\frac{\delta t_m}{t_m}\right)^2\right]^{1/2} \tag{2.3}$$

where :

δN : Error on the absorption peak intensity

δA : error on the source activity

$\delta\gamma$: error on the branching ratio

δt_m : error on the counting time

Using the energies taken we calculate the efficiency the results are shown in the following table:

Table 2.3: Values of efficiency Vs gamma ray

Source	Energy (KeV)	Efficiency (%)	Error (%)	I_γ
Am-241	59.54	1.52×10^{-3}	0.48	35.94
Ba-133	81.04	1.82×10^{-3}	1.30	34.06
	276.39	4.524×10^{-3}	1.27	7.16
	302.85	4.23×10^{-3}	1.21	18.33
	356.02	3.61×10^{-3}	1.10	62.05
	383.84	3.31×10^{-3}	1.20	8.93
Co-60	1173.24	1.21×10^{-3}	0.42	99.97
	1332.50	1.11×10^{-3}	0.43	99.98
Cs-137	661.65	2.042×10^{-3}	0.52	85.12
Eu-152	121.83	6.83×10^{-3}	0.84	28.58
	244.71	5.22×10^{-3}	0.92	7.58
	344.27	3.74×10^{-3}	0.79	26.54
	411.13	3.31×10^{-3}	0.96	2.23
	778.88	1.78×10^{-3}	0.88	12.94
	964.01	1.46×10^{-3}	0.82	14.60
	1112.08	1.28×10^{-3}	0.85	13.64
	1408.16	1.08×10^{-3}	0.83	21.01

Using the previous table we can conclude the following graphe obtained by Genie2000 showing the different ranges in efficiency by the energies :

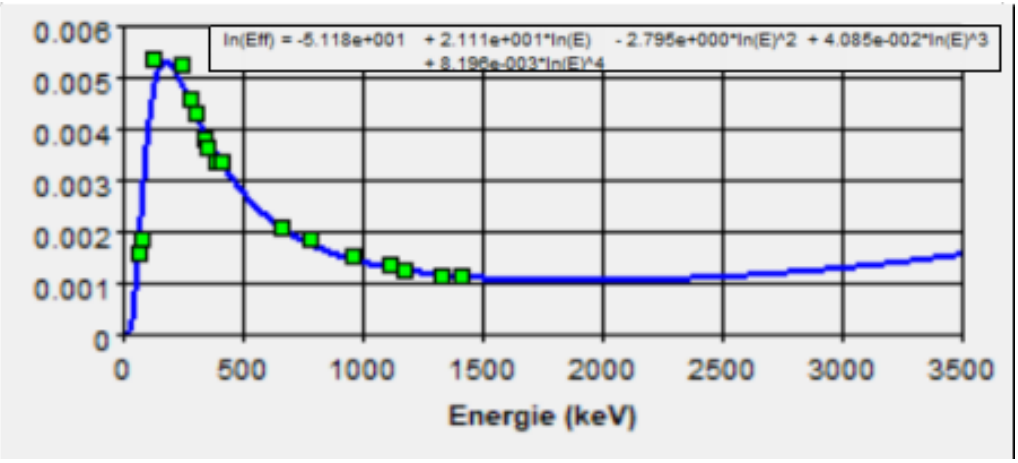

Figure 2.6: Calibration line of Efficiency by different energies using Genie 2K software [67]

The Figure 2.6 illustrates the calibration curve of detection efficiency as a function of energy levels, using Genie 2k software. The x-axis represents energy in keV (kilo-electron volts), and the y-axis indicates the detection efficiency. The measured data points show efficiencies at specific energy levels, including significant points around 0 to 500 keV, where the efficiency is highest and decreases rapidly. Beyond 500 keV, the efficiency levels off and remains relatively constant up to 3500 keV. The line represents a fitted curve, described by a polynomial equation, that models the detector's efficiency response across these energy levels, crucial for accurate gamma spectroscopy analysis.

The energy and efficiency calibration data will be used as input in the measurement section presented in Chapter 3. These calibrated parameters are essential for ensuring the accuracy and reliability of the measurements conducted throughout the study.

The software Genie 2k takes in consideration many equations such as Energy, Full Width Half Maximum (FWHM), Low Tail, which they are important for for detector calibratrion. The resolution provides separation for two adjacent energy peaks, which leads to the identification of different radionuclides in the spectrum. It can be defined as the power to separate the energy peaks in the spectrum. The energy resolution of the detector was determined by calculating the full width at half-maximum (FWHM) of the peaks.

$$R = \frac{FWHM}{E_0}.100 \tag{2.4}$$

R is the energy resolution of the detector, and E_0 is the energy of the peak center of the related radionuclide [69].

2.4 Summing Effect Correction

In the experiment to determine the referential distance for negligible summing effects using Co-60, various distances were tested. At a distance of D0 = 0 cm and D1 = 2.2 cm, the summing effect was found to be not negligible. However, at a distance of D2 = 4.4 cm, the summing effect was negligible. These results indicate that the summing effect decreases with increasing distance from the Co-60 source, becoming negligible at 4.4 cm. This referential distance is critical for accurate measurements in gamma spectroscopy, ensuring that the summing effect does not interfere with the observed spectral data.

Chapter 3

Experimental Findings and Analysis

In this chapter, we will explor the experimental aspect of our research, focusing on three medicinal plants: Laurus nobilis (bay laurel), Pistacia lentiscus (mastic tree), and Rosmarinus officinalis (rosemary). These plants have been selected due to their renowned therapeutic properties and their significance in traditional medicine. Our primary objective is to perform a detailed analysis of their elemental composition using the k_0-Standardized Neutron Activation Analysis (k_0-NAA) technique. This method allows us to accurately quantify both essential and non-essential elements present in the plant samples. By applying k_0-NAA, we aim to obtain precise data on the concentrations of various elements, which can contribute to understanding the medicinal properties and potential health benefits of these plants. The findings from this analysis could provide valuable insights into the nutritional and pharmacological profiles of Laurus nobilis, Pistacia lentiscus, and Rosmarinus officinalis, further supporting their use in modern and traditional therapeutic applications.

3.1 Material and Methods

3.1.1 Material

3.1.1.1 Plants

The three plant species were sourced from a reputable nursery to ensure the consistency and quality of the samples. Below is an image depicting the plants in their nursery environment, illustrating the conditions in which they were grown prior to analysis.

Figure 3.1: Plant Sampling: Laurel, Rosemary, and Pistacia Respectively

The nursery is located in the mayoralty of Soumaa, 9.04 Km from Blida. The map below provides a visual representation of the nursery's location within Blida.

Figure 3.2: Geographical Locations of Plant Collection [70]

3.1.1.2 Standard References

Certified reference materials are used for calibration and validation, and high-purity reagents along with distilled water are employed for sample preparation. We used SRM-NIST1573a (tomato leaves) and CRM-GSV4 (tea leaves).

Figure 3.3: Certified Reference Materials Utilized in this Study

3.1.1.3 Other Lab Tools

various lab tools were used, including an analytical scale for precise weighing, sieves for particle size separation, and a porcelain grinder for homogenizing the plant samples into a fine powder.

Figure 3.4: other tools used in the study : oven, analytical scale

3.1.1.4 Gold Monitor

Gold (Au) monitors in the k_0-Neutron Activation Analysis technique are composed of 99.9% aluminum and 0.1% gold. This specific composition ensures even distribution of gold within the aluminum matrix, facilitating precise neutron activation and accurate radioactivity measurement. During k_0-NAA, samples and gold-aluminum monitors are irradiated with neutrons, transforming gold atoms into radioactive isotopes, primarily Au-198 (half-life of 2.7 days),

which are measured via gamma spectroscopy.
The aluminum matrix supports the gold and acts as a neutron moderator, optimizing neutron capture by gold. Using high-purity aluminum minimizes interference from other elements, ensuring accurate gamma-ray emission measurements from gold isotopes. Gold is chosen because it is more appropriate for several reasons: it does not interfere with gamma-ray lines, has no coincidence peaks, no sum peaks, no single escape or double escape peaks, due to its gamma rays emission that is ≤ 1022 keV. This precise composition is crucial for k_0-NAA as it allows accurate characterization of neutron flux, essential for comparing induced radioactivities of sample elements to the gold standard. The reliable neutron capture properties of gold make it an ideal standard for k0-NAA. [71].

3.1.1.5 Reactor

In algeria, there is two nuclear reactors, Es-salem in Birine, Djelfa (15 MW) and NUR (1 MW) in Draria, used for research. The NUR reactor, located at the Nuclear Research Centre of Draria (CRND) in Algiers, is a pool-type research reactor that uses low-enriched uranium (LEU) as fuel. Commissioned in the 1980s. The reactor is pivotal for training nuclear engineers and scientists, operating under the supervision of the Commissariat à l'Énergie Atomique (COMENA) and in collaboration with the International Atomic Energy Agency (IAEA) to ensure stringent safety standards [72].

3.1.1.6 Softwares

The analysis and processing of data utilized a range of specialized software tools, including HyperLab 2023, KayWin 2024, KayZero for Windows V4.04, and Genie 2k. HyperLab 2023 excels in multidimensional data analysis and visualization, particularly beneficial for handling complex datasets. KayWin 2024 provided a user-friendly interface and comprehensive data management functionalities, ensuring efficient data handling and organization. KayZero for Windows V4.04 contributed expertise in zero-crossing analysis and peak fitting, enhancing the precision of spectral interpretation and data refinement. Genie2K complemented these tools with its capabilities in gamma spectroscopy and nuclear counting applications, facilitating robust spectrum analysis and data processing throughout the study. Together, these software resources enabled thorough analysis and detailed characterization of the dataset.

3.1.2 Methods

3.1.2.1 k_0 Standardization

In adherence to k_0-NAA principles outlined in Chapter 1, the study will utilize established k_0 factors and neutron flux parameters to quantitatively determine elements of interest, ensuring accuracy and reliability in the analysis process.

3.1.2.2 Sampling and Samples Preparation

After collecting the leaves of Laurel (Laurus nobilis), Pistacia (Pistacia Lentiscus), and Rosemary (Rosmarinus officinalis), they were thoroughly rinsed with distilled water multiple times. The leaves were then placed in an oven set to 40°C and dried for two hours. Subsequent to the drying process, we proceeded to the laboratory, sterile environment. The dried leaves were then transferred to a porcelain mortar and pestle for grinding. As illustrated in Figure 4, the grinding process commenced with the Pistacia leaves.

Figure 3.5: Grinding process

Lastly, we proceeded to the sieving phase, utilizing a 200 µm filter to remove larger particles from our samples. The processed samples were then placed in clean containers, ready for further analysis.

Figure 3.6: Sieving process

3.1.2.3 Irradiation

Short Irradiation

The prepared samples were placed in polyethylene capsules. Initially, the empty capsules were weighed using a digital balance. Subsequently, the samples were added to the capsules using a spatula, with each sample massing approximately 200 mg.

We prepared two samples for each medicinal plant, assigning the following codes: Laurel (L1 and L2), Pistacia (P1 and P2), and Rosemary (R1 and R2). The standards used were GSV4 (Tea leaves), coded as St1 and St2, and NIST1573a (Tomato leaves), coded as St3 and St4. The final prepared samples are shown in figure (3.7).

Figure 3.7: Final prepared samples for short irradiation

Medium And Long Irradiation

The samples were placed in pure aluminum capsules. The capsules were prepared by sealing the sides, leaving only one opening for sample insertion. Initially, the empty capsules were weighed, with masses around 45 mg. After adding the samples and sealing the capsules, the total masses were approximately 100 mg. Similar to the short irradiation samples, we prepared two samples for each medicinal plant with the following codes: Laurel (LL1 and LL2), Pistacia (LP1 and LP2), and Rosemary (LR1 and LR2).

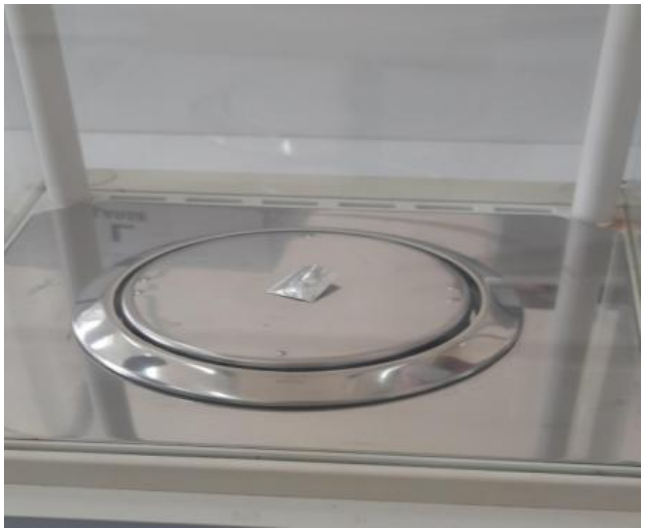

Figure 3.8: Aluminum capsules

We resumed the expected isotopes, their half lives, natural abundance and analytical photopeaks in table 3.1 [73]

Table 3.1: Isotopic Characteristics

Initial element	**Nat. Abundance (%)**	**Product isotope**	**Half-life**	**Analytical photopeaks [Kev]**	k_0 **factor**
Ca	96.941	Ca-48	4.3×10^{19}y	489.2	9.14×10^{-8}
K	93.2581	K-42	1.25×10^{9}y	312.7	1.59×10^{-5}
Mg	78.99	Mg-27	$9.458 mins$	170.7	3.02×10^{-6}
Cl	75.53	Cl-38	3.01×10^{5}y	1642.7	1.97×10^{-3}
Na	100	Na-24	15 h	1368.6	4.68×10^{-2}
Fe	91.754	Fe-59	44.5d	142.7	1.33×10^{-6}
Mn	100	Mn-56	2.5785h	846.8	4.96×10^{-1}
Zn	49.839	Zn-65	244d	1115.5	5.72×10^{-3}
Cr	100	Cr-51	27.7d	320.1	2.62×10^{-3}
Co	100	Co-60	5.27y	1173.2	1.32
V	99.75	V-52	3.74min	1434.1	1.96×10^{-1}
Br	50.69	Br-80	17.7min	616.6	6.92×10^{-3}
Ba	100	Ba-131	11.5d	123.8	3.78×10^{-5}

Continued on next page

Table 3.1: Isotopic Characteristics (continued)

Initial element	**Nat. Abundance (%)**	**Product isotope**	**Half-life**	**Analytical photopeaks [Kev]**	k_0 **factor**
Gd	20.47	Gd-153	240.4d	97.4	5.86×10^{-3}
Ce	100	Ce-141	32.5d	145.4	3.66×10^{-3}
Rb	72.17	Rb-83	86.2d	1077	7.65×10^{-4}
Tm	100	Tm-170	128.6d	84.3	3.26×10^{-2}
La	99.91	La-140	1.68d	328.8	2.87×10^{-2}
Th	100	Pa-233	21.83y	300.1	4.37×10^{-3}
Sc	100	Sc-46	84d	889.3	1.22
Sb	100	Sb-124	60.20d	564.2	4.38×10^{-2}
Hf	100	Hf-175	70.65d	343.4	9.06×10^{-3}
Cs	100	Cs-134	2.0652y	563.2	3.98×10^{-2}
Eu	52.2	Eu-152	13.54y	121.8	1.28×10^{1}
Sm	100	Sm-153	46.3h	69.7	3.52×10^{-2}
Ta	99.988	Ta-182	114.4d	67.8	9.08×10^{-2}
Tb	100	Tb-160	72.3 d	86.8	4.20×10^{-2}
Sr	82.58	Sr-85	64.9d	514	6.92×10^{-5}
Al	100	Al-28	2.245min	1778.9	1.75×10^{-2}
Zr	28.99	Zr-95	64d	724.2	8.90×10^{-5}

The Table 3.1 offers a comprehensive overview of various initial elements, their natural abundances, product isotopes, half-lives, analytical photopeaks, and k_0 factors. Elements such as Mn, Zn, Cr, Co, V, Br, Ba, Gd, Ce, Rb, Tm, La, Th, Sc, Sb, Hf, Cs, Eu, Sm, Ta, Tb, Sr, Al, and Zr

are detailed with their natural abundances ranging from 20.47% for Gd to 100% for several others like Mn, Cr, Co, and La. Each element's product isotope is listed along with its half-life, varying from as short as 6.0×10^{-7} seconds for V-52 to as long as 1.82×10^{15} years for Ta-182. The analytical photopeaks are given in KeV, indicating the energy levels at which these isotopes can be detected, such as 846.8 KeV for Mn-56 and 1173.2 KeV for Co-60. The k_0 factors, which are crucial for neutron activation analysis, range from 1.75×10^{-2} for Al-28 to 4.96×10^{-1} for Mn-56. This detailed data is essential for applications in nuclear science and materials analysis.

Table 3.2: Irradiation and Measurement Parameters

Irradiation	Short	Medium	Long
Channel	Pneumatic system	Vertical channel	
α	-0.02257	-0.0059	
f	21.9	20.7	
$T_i(s)$	100	14400	
T_d	5-213 min	5 d	15 d
$T_m(s)$	300, 1200	first meas (3600)	second meas (10800)
Elements	Al, Br, Ca, Cl, K, Mg, Mn, Na, Sr, V	Ba, Br, Ca, Ce, Co, Cr, Cs, Eu, Fe, Gd, Hf, K, La, Na, Rb, Sb, Sc, Sm, Sr	Ba, Ce, Co, Cr, Cs, Eu, Fe, Gd, Hf, K, La, Na, Rb, Sb, Sc, Sm, Sr, Ta, Tb, Th, Tm, Zn, Zr

The table presents a comparison of short, medium, and long irradiation periods, specifying the channels used, their parameters, and the elements detected in each period. For short irradiation, a pneumatic system channel is used with an alpha value of -0.02257 and an f factor of 21.9, an irradiation time T_i of 100 seconds, a decay time T_d ranging from 5 to 213 minutes, and measurement times T_m of 300 and 1200 seconds. The elements detected in this period include Al, Br, Ca, Cl, K, Mg, Mn, Na, Sr, and V. Medium irradiation uses a vertical channel with an irradiation time of 14400 seconds (4 hours), a decay time of 5 days, and a measurement time of 3600 seconds (1 hour), detecting elements such as Ba, Br, Ca, Ce, Co, Cr, Cs, Eu, Fe, Gd, Hf, K, La, Na, Rb, Sb, Sc, Sm, and Sr. Long irradiation also uses a vertical channel with an alpha value of - 0.0059 and an f factor of 20.7, an irradiation time of 14400 seconds (4 hours), a decay time of 15 days, and a measurement time of 10800 seconds (3 hours), detecting elements including Ba, Ce, Co, Cr, Cs, Eu, Fe, Gd, Hf, K, La, Na, Rb, Sb, Sm, Ta, Tb, Th, Tm, Zn, and Zr.
the parameters of Table 3.1 and 3.2 will be involved in the calculation of element concentrations

3.1.2.4 Decay Time

After irradiation, the samples are allowed to cool to reduce the radioactivity to manageable levels. The cooling time varies depending on the half-lives of the activated isotopes.For short irradiation the decay time varied from 5 to 213 minutes, while medium irradiation around 5 days, and long irradiation around 15 dzys, as showing in Table 3.2.

3.1.2.5 Measurement

Before performing calculations, the spectra (Fig. 3.9) are processed using HyperLab, which generates two data files: PTF and SPE. These files are then imported into KayWin for further analysis or utilized as input data within KayWin's software environment. This sequential process ensures that the spectral data is prepared and formatted appropriately before conducting detailed calculations and analyses in subsequent stages of the study.

In the measurement phase, we used an HPGe detector (30%) coupled with a spectrometry chain to perform the detection. The gamma spectra were analyzed using Genie2k software, ensuring precise identification and quantification of the elements present in the plant samples. Multiple measurements were taken at different cooling intervals (300s, 1200s for short irradiation and 3600s, 10800s for long irradiation) to capture isotopes with varying half-lives. The k_0-NAA method involves key parameters such as the alpha (α) factor, accounting for the epithermal neutron flux distribution, and the f factor, representing the thermal to epithermal neutron flux ratio, both crucial for accurate quantification.

The figure 3.9 shows the measured gamma spectra.

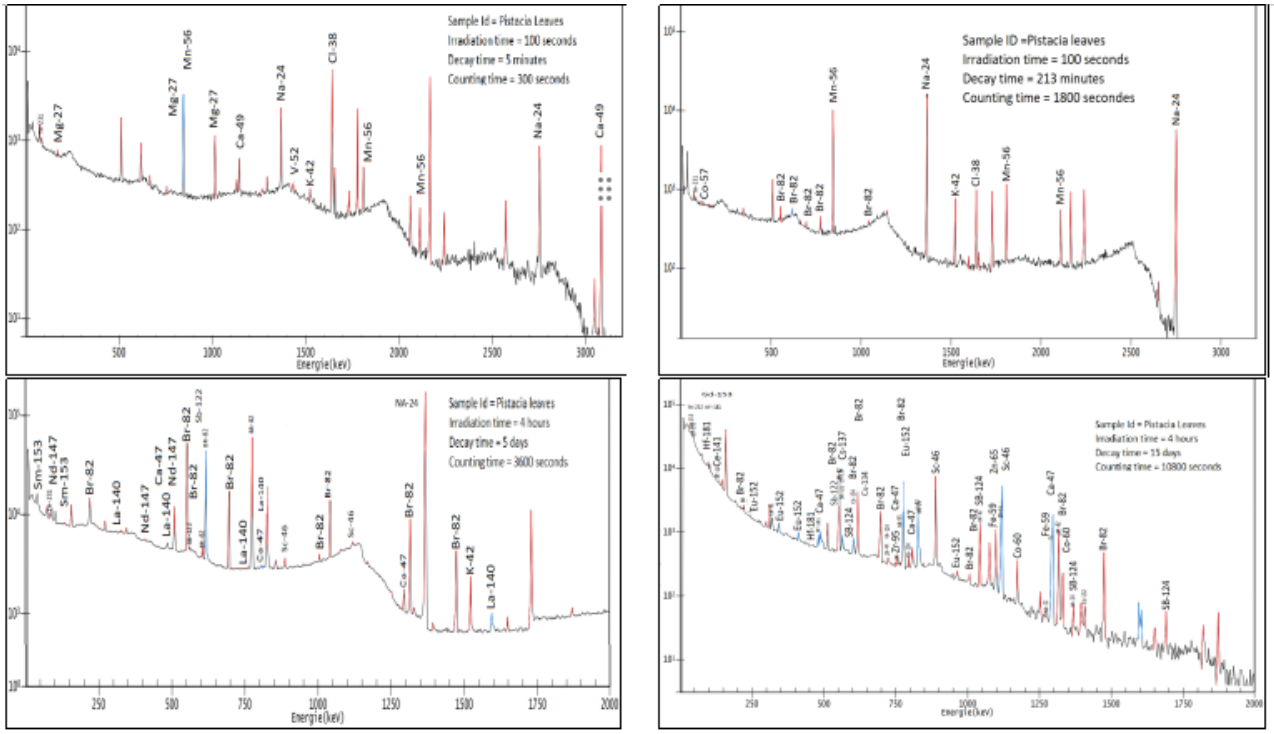

Figure 3.9: Gamma-Ray Spectra of Pistacia Leaf Samples: 100 Seconds and 4 Hours Irradiation, with Cooling Times from 5 Minutes to 15 Days, Measured for 300s, 1800s, 3600s, and 10800s Using Genie2k software

The provided spectra illustrate the gamma-ray activity in Pistacia leaf samples under var-

ious irradiation and cooling conditions, showcasing the impact of irradiation duration and cooling time on the isotopic composition of the samples. Each peak in the spectra corresponds to specific isotopes and their energy levels, reflecting the complex interplay of irradiation time, cooling time, and isotopic composition of the samples.

Short lived determination

Short Cooling Times: For spectra obtained shortly after a 100-second irradiation, peaks corresponding to short-lived isotopes are prominent. Notable isotopes include Al-28 and Mn-56, which have relatively short half-lives of 2.24 minutes and 2.58 hours, respectively. These isotopes exhibit high-intensity peaks due to their rapid decay post-irradiation.

Long Cooling Times: As the cooling time increases, the intensity of peaks associated with short- lived isotopes like Al-28 and Mn-56 diminishes significantly. This results in the spectra highlighting longer-lived isotopes such as Na-24 and K-42, with half-lives of 15 hours and 12.36 hours respectively, indicating a shift in the isotopic activity.

Medium and long determination

Short Cooling Times: With a 4-hour irradiation, the spectra obtained after short cooling times show higher intensity peaks compared to the shorter irradiation period. This is due to the increased production of isotopes through prolonged neutron activation. Prominent isotopes include Na-24, Mn-56, and Br-82, with Br-82 having a half-life of 35.3 hours, contributing significantly to the detected gamma-ray activity.

Long Cooling Times: For long cooling times post a 4-hour irradiation, the spectra reveal the decay of short-lived isotopes, with residual peaks primarily representing longer-lived isotopes such as Zn-65 (half-life of 244 days) and Co-60 (half-life of 5.27 years). The gradual decrease in peak intensity for short-lived isotopes allows for the identification and analysis of these long-lived isotopes. Major Detected Isotopes Across the different spectra, the major isotopes detected include Na-24, Mn-56, K-42, Al-28, Br-82, Zn-65, and Co-60. These isotopes are products of neutron activation in the Pistacia leaf samples and are indicative of the elemental composition, reflecting the presence of elements like Ca-47, Na-24, Mn-56, Sm-153, K-42, Mg-27, Br-82, Eu-152, V-52,Nd-147 and La-140.

The gamma-ray spectra provide valuable insights into the isotopic composition of Pistacia leaves, demonstrating the effect of irradiation and cooling times on the detectable isotopes. The presence of both short-lived and long-lived isotopes highlights the dynamic changes in isotopic activity, crucial for understanding the elemental and isotopic behavior under neutron activation.

3.1.2.6 Calculation

In the calculation phase, the gamma spectra obtained from the HPGe detector were initially processed using HyperLab 2023 software, which facilitated precise peak identification and spectrum analysis. Following this, the data were further analyzed to calculate element concentrations using KayWin 2024 and KayZero for Windows V4.04. These software tools were instrumental in applying the k_0-standardization method, accounting for critical factors such as neutron flux variations, self-shielding effects, and the key parameters α and f presented in Table 3.2. The integration of these advanced software solutions ensured a high level of accuracy and reliability in the quantification of both essential and non-essential elements present in the plant samples.

3.1.2.7 Validation and quality control

The statistical analysis includes calculating Z-scores and U-scores during the data analysis phase to validate the results. Z-scores assess the accuracy by determining how far a result deviates from the expected value in terms of standard deviations, while U-scores evaluate the precision by measuring the uncertainty of the measurement. Below are Z-scores and U-scores expressions respectively [3] :

$$Zscore = \frac{C_m - C_c}{\mu_c} \tag{3.1}$$

If :

$$\begin{cases} -2 < Zscore < 2 & \text{accepted} \\ 2 < |Zscore| < 3 & \text{questionable} \\ |Zscore| > 3 & \text{rejected} \end{cases}$$

$$Uscore = \frac{|C_m - C_c|}{\sqrt{\mu_m^2 + \mu_c^2}} \tag{3.2}$$

if :

$$\begin{cases} U \leq 1 & \text{accepted} \\ \text{Other} & \text{rejected} \end{cases}$$

Where :

C_c : certified concentration

C_m : measured concentration

μ_c : certified standard deviation

μ_m : measured standard deviation

The following table summarizes the measured concentrations, certified concentrations, and associated errors of elements found in our laurel, pistacia, and rosemary samples.

Table 3.3: Evaluation using GSV4 and NIST1573a

Element	unit	CRM-GSV4				SRM-NIST1573a			
		This work	Certified value	Zscore	Uscore	This work	Certified value	Zscore	Uscore
Al	%	0.300 ± 0.023	0.300 ± 0.045	0	0	0.0592 ± 0.004	0.06 ± 0.0007	0.90	0.16
Ca	%	0.460 ± 0.070	0.430 ± 0.040	-0.75	0.37	4.76 ± 0.13	5.045 ± 0.055	5.18	2.02
Cl	%	0.038 ± 0.003				0.664 ± 0.047	0.66 ± 0.099	-0.04	0.04
K	%	1.740 ± 0.310	1.660 ± 0.120	-0.67	0.24	2.67 ± 0.25	2.676 ± 0.048	0.13	0.02
Mg	%	0.180 ± 0.010	0.170 ± 0.020	-0.50	0.45	1.18 ± 0.1	1.2 ± 0.18	0.11	0.10
Mn	%	0.124 ± 0.013	0.124 ± 0.007	-0.06	0.03	0.0246 ± 0.002	0.025 ± 0.001	0.03	0.01
As	mg/kg	0.284 ± 0.052	0.28 ± 0.04	-0.10	0.06	0.112 ± 0.004	0.113 ± 0.002	0.25	0.13
Ba	mg/kg	58.86 ± 2.1	58 ± 6	-0.14	0.14	64 ± 5	63 ± 9.45	-0.11	0.09
Br	mg/kg	3.437 ± 0.9	3.4 ± 0.5	-0.07	0.04	1149 ± 13	1300 ± 195	0.77	0.77
Ce	mg/kg	1.007 ± 0.041	1 ± 0.2	-0.03	0.03	1.79 ± 0.18	2 ± 0.3	0.70	0.60
Co	mg/kg	0.196 ± 0.02	0.18 ± 0.02	-0.80	0.57	0.569 ± 0.06	0.577 ± 0.007	1.17	0.14
Cr	mg/kg	0.85 ± 0.04	0.8 ± 0.03	-1.67	1.00	2.01 ± 0.02	1.988 ± 0.034	-0.65	0.56
Cs	mg/kg	0.302 ± 0.014	0.28 ± 0.02	-1.10	0.90	0.051 ± 0.008	0.053 ± 0.008	0.25	0.18
Eu	mg/kg	0.01837 ± 0.0058	0.018 ± 0.002	-0.19	0.06				
Fe	mg/kg	258 ± 9.31	264 ± 15	0.40	0.34	365 ± 17	367.5 ± 4.3	0.58	0.14
La	mg/kg	0.524 ± 0.07	0.6 ± 0.04	1.90	0.94	2.5 ± 0.2	2.3 ± 0.345	-0.58	0.50
Na	mg/kg	45 ± 7	44 ± 6	-0.17	0.11	136 ± 11	136.1 ± 3.7	0.03	0.01
Rb	mg/kg	70 ± 1.5	74 ± 5	0.80	0.77	14.61 ± 0.83	14.83 ± 0.31	0.71	0.25
Sb	mg/kg	0.05734 ± 0.01	0.056 ± 0.006	-0.22	0.11	0.063 ± 0.006	0.062 ± 0.003	-0.34	0.16
Sc	mg/kg	0.078 ± 0.008	0.085 ± 0.013	0.54	0.46	0.09 ± 0.01	0.1 ± 0.015	0.67	0.55
Sm	mg/kg	0.09238 ± 0.005	0.085 ± 0.023	-0.32	0.31	0.26 ± 0.09	0.19 ± 0.029	-2.46	0.74
Sr	mg/kg	13.9 ± 1.5	15.2 ± 0.7	1.86	0.79	99 ± 15	85 ± 12.75	-1.10	0.71
Tb	mg/kg	0.01076 ± 0.006	0.011 ± 0.00165	0.15	0.04				
Th	mg/kg	0.06237 ± 0.005	0.061 ± 0.009	-0.15	0.13	0.114 ± 0.004	0.12 ± 0.018	0.33	0.33
Yb	mg/kg	0.04675 ± 0.015	0.044 ± 0.005	-0.55	0.17				
Zn	mg/kg	27.29 ± 3.13	26.3 ± 2	-0.49	0.27	29.95 ± 0.9	30.94 ± 0.55	1.80	0.94

The next histogram visually represents the results presented in the previous table.

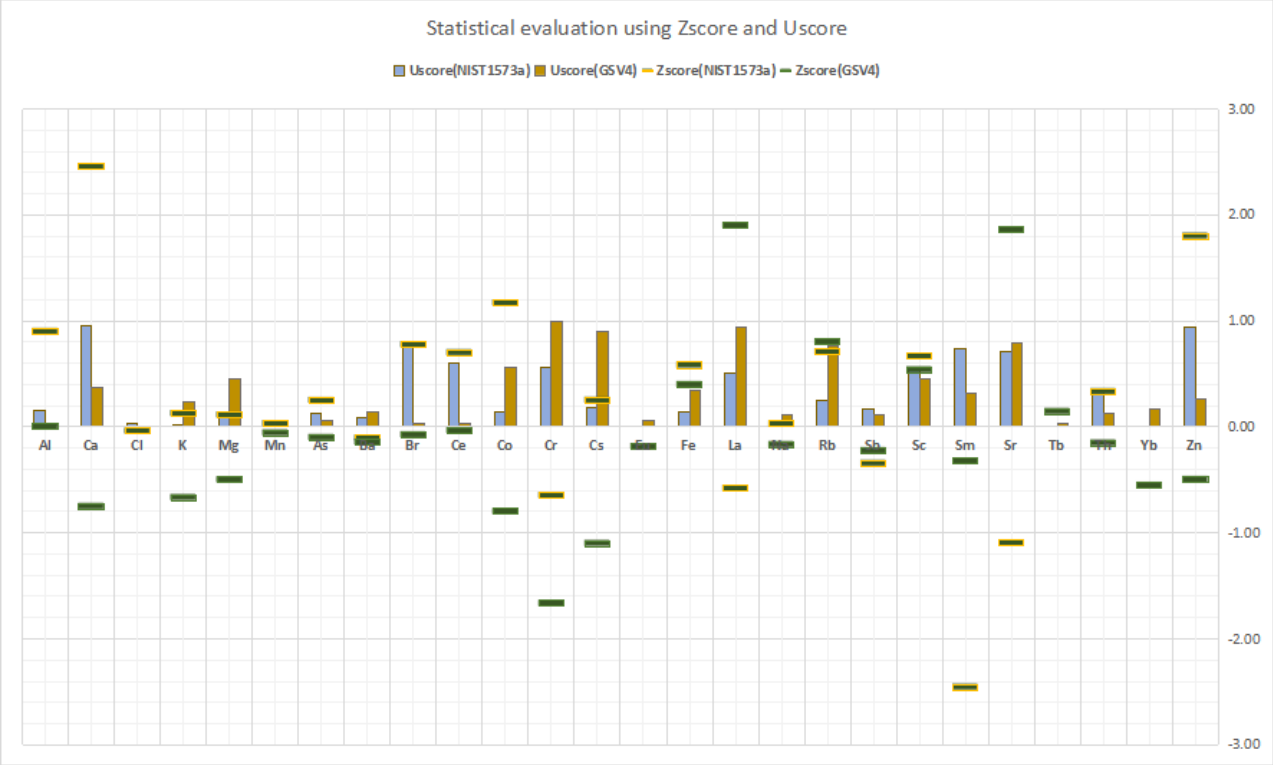

Figure 3.10: Evaluation of results using Zscore and Uscore

The provided data compares the values obtained in our work with certified values GSV4 and NIST1573a, where calculating the Z-score and U-score for validation purposes. For most elements, such as Al, K, Mg, Mn, As, Ba, Br, Ce, Co, Cr, Cs, Eu, Fe, Na, Rb, Sb, Sc, Tb, Th, Yb, and Zn, the Z-scores fall within the -2 to 2 range, indicating that the results are acceptable.

Similarly, the U-scores for these elements are also ≤ 1, further validating the accuracy and precision of the measurements.

However, there are exceptions where the results do not meet the acceptance criteria.

For instance, Calcium (Ca) shows a Z-score of 5.18 and a U-score of 2.02, both of which are beyond acceptable limits, indicating a significant discrepancy from the certified values and lack of precision in the results. Similarly, elements such as Br and Sm have U-scores of 0.77 and 0.74 respectively, which are within acceptable limits, but still on the higher end indicating potential concerns. For elements like Sr and Zn, Z-scores are 1.86 and 1.80 respectively, and although they are within acceptable limits, they are relatively high and warrant close attention.

3.2 Results and discussion

We successfully analyzed 30 elements using Kaywin 2024 software, in the Laurel, Pistacia, and Rosemary samples, categorizing them into Essential-macrominerals (E.mac), Essential microminerals (E.mic), and Non-Essential Elements (N.E). The Essential Elements detected include Ca, K, Mg, Cl, Na, Fe, Mn, Zn, Cr, Co, and V, which are vital for various biological functions and plant health. Non-essential elements such as Br, Ba, Gd, Ce, Rb, Tm, La, Th, Sc, Sb, Hf, Cs, Eu, Sm, Ta, Tb, Sr, Al, and Zr were also identified, providing insights into environmental influences and potential accumulation in the plants.
The table 3.4 summarizes the results of our elemental analysis.

Essential Macrominerals

The concentrations of essential macrominerals in Laurel, Pistacia, and Rosemary reveal notable variations.
Calcium (Ca), critical for bone health, muscle function, and nerve signaling, is highest in Pistacia (4.54 %) compared to Laurel (1.653 %) and Rosemary (0.95 %). This high level in Pistacia can be beneficial for individuals looking to increase their calcium intake through natural sources.
Potassium (K), important for maintaining fluid balance, nerve transmission, and muscle contraction, is most abundant in Rosemary (1.47 %), followed by Laurel (0.469 %) and Pistacia (0.376 %). Adequate potassium intake is essential for cardiovascular health, and Rosemary appears to be a particularly rich source.
Magnesium (Mg), necessary for over 300 biochemical reactions in the body, including energy production and DNA synthesis, is most concentrated in Pistacia (0.589 %), with lower levels in Laurel (0.234 %) and Rosemary (0.201 %). Magnesium supports muscle and nerve function, blood glucose control, and blood pressure regulation.
Chlorine (Cl), part of the essential electrolyte chloride, which helps maintain fluid balance and is crucial for digestive health, is highest in Pistacia (0.79 %), compared to Laurel (0.164 %) and Rosemary (0.242 %).
Sodium (Na), crucial for maintaining fluid balance, nerve function, and muscle contractions, is fairly consistent across the samples, with Pistacia having a slightly higher concentration (0.19) than Laurel (0.114 %) and Rosemary (0.107 %).

Table 3.4: Concentration values of essential macro, micro, and non essential elements obtained by k_0 in Pistacia, Laurel, and Rosemary using Kaywin software

	Element	Unit	Laurel		2σ	Pistacia		2σ	Rosemary		2σ
E.mac	Ca	%	1.653	±	0.046	4.54	±	0.46	0.95	±	0.1
	K	%	0.469	±	0.042	0.376	±	0.022	1.47	±	0.07
	Mg	%	0.234	±	0.02	0.589	±	0.048	0.201	±	0.019
	Cl	%	0.164	±	0.013	0.79	±	0.07	0.242	±	0.02
	Na	%	0.114	±	0.009	0.19	±	0.015	0.107	±	0.0049
E.mic	Fe	mg/kg	381	±	10	328	±	21	548	±	29
	Mn	mg/kg	48.3	±	3.5	25.6	±	1.9	16.9	±	1.4
	Zn	mg/kg	41.2	±	0.8	26.8	±	3.2	47	±	8
	Cr	mg/kg	13.8	±	0.7	1.41	±	0.1	2.13	±	0.35
	Co	mg/kg	0.242	±	0.024	0.219	±	0.012	0.297	±	0.012
	V	mg/kg	-		-	0.37	±	0.12	0.62	±	0.14
N.E	Br	mg/kg	12.65	±	0.07	38.04	±	0.21	7.585	±	0.047
	Ba	mg/kg	11.8	±	3.4	10.1	±	1.8	29	±	2.6
	Gd	mg/kg	-		-	6.7	±	1.1	5.7	±	0.9
	Ce	mg/kg	3	±	0.2	1.57	±	0.23	1.84	±	0.24
	Rb	mg/kg	1.95	±	0.21	5.7	±	0.6	14.8	±	1.6
	Tm	mg/kg	1.05	±	0.12	1.85	±	0.16	-		-
	La	mg/kg	0.27	±	0.022	0.16	±	0.06	0.253	±	0.026
	Th	mg/kg	0.268	±	0.015	0.242	±	0.009	0.275	±	0.012
	Sc	mg/kg	0.259	±	0.018	0.212	±	0.007	0.163	±	0.007
	Sb	mg/kg	0.206	±	0.014	0.105	±	0.008	0.133	±	0.011
	Hf	mg/kg	0.105	±	0.009	0.081	±	0.001	0.226	±	0.024
	Cs	mg/kg	0.059	±	0.01	0.085	±	0.013	0.08	±	0.009
	Eu	mg/kg	0.0428	±	0.0024	0.0325	±	0.0026	0.0504	±	0.0039
	Sm	mg/kg	0.0384	±	0.0018	0.0363	±	0.0029	0.0716	±	0.0035
	Ta	mg/kg	-		-	-		-	0.086	±	0.016
	Tb	mg/kg	-	±	-	-	±	-	0.253	±	0.036
	Sr	mg/kg	345	±	27	95	±	8	103	±	8
	Al	mg/kg	306	±	24	286	±	21	393	±	28
	Zr	mg/kg	41	±	7	-		-	-		-

Essential Microminerals

The data for essential microminerals highlight important differences across the three plants. Iron (Fe), vital for the production of hemoglobin and myoglobin, which carry oxygen in the blood and muscles, is most concentrated in Rosemary (548 mg/kg), followed by Laurel (381 mg/kg) and Pistacia (328 mg/kg). Iron is crucial for preventing anemia and supporting overall energy levels.

Manganese (Mn), a cofactor for many enzymes involved in metabolism, bone formation, and antioxidant function, shows the highest concentration in Laurel (48.3 mg/kg), with lower levels in Pistacia (25.6 mg/kg) and Rosemary (16.9 mg/kg).

Zinc (Zn), essential for immune function, protein synthesis, and DNA synthesis, is most abundant in Rosemary (47 mg/kg), with Laurel (41.2 mg/kg) and Pistacia (26.8 mg/kg) containing lower amounts. Zinc supports immune health and wound healing.

Chromium (Cr), involved in carbohydrate, fat, and protein metabolism, shows a high concentration in Laurel (13.8 mg/kg), whereas Pistacia (1.41 mg/kg) and Rosemary (2.13 mg/kg) have significantly lower levels. While small amounts of chromium are necessary, high levels can be toxic.

Cobalt (Co), a component of vitamin B12, has relatively similar concentrations across the plants, with Laurel (0.242 mg/kg), Pistacia (0.219 mg/kg), and Rosemary (0.297 mg/kg) showing minor differences. Cobalt is crucial for preventing vitamin B12 deficiency anemia.

Vanadium (V) is present in Pistacia (0.37 mg/kg) and Rosemary (0.62 mg/kg), with no data for Laurel. The role of vanadium in human nutrition is less clear, but it is considered to have potential insulin-mimetic properties.

Non Essential Elements

NEE also exhibit distinct patterns among the plants. Bromine (Br), used in flame retardants and with no established biological role in humans, is highly concentrated in Pistacia (38.04 $\pm$ 0.21 mg/kg), significantly higher than in Laurel (12.65 $\pm$ 0.07 mg/kg) and Rosemary (7.585 $\pm$ 0.047 mg/kg).

Barium (Ba), which has some industrial applications but no known biological role, is highest in Rosemary (29 $\pm$ 2.6 mg/kg), with lower concentrations in Laurel (11.8 $\pm$ 3.4 mg/kg) and Pistacia (10.1 $\pm$ 1.8 mg/kg).

Gadolinium (Gd), used in medical imaging, is found in Pistacia (6.7 $\pm$ 1.1 mg/kg) and Rosemary (5.7 $\pm$ 0.9 mg/kg), with no data for Laurel.

Cerium (Ce), used in various industrial applications, is most concentrated in Laurel (3 $\pm$ 0.2 mg/kg) compared to Pistacia (1.57 $\pm$ 0.23 mg/kg) and Rosemary (1.84 $\pm$ 0.24 mg/kg).

Rubidium (Rb) levels are highest in Rosemary (14.8 $\pm$ 1.6 mg/kg), with lower amounts in

Pistacia (5.7 ± 0.6 mg/kg) and Laurel (1.95 ± 0.21 mg/kg).
Thulium (Tm) and Lanthanum (La) show varying concentrations, with the highest values observed in Pistacia and Rosemary.
Thorium (Th) levels are comparable across all plants.
Scandium (Sc) is highest in Laurel (0.259 ± 0.018 mg/kg), and the concentrations of antimony (Sb), hafnium (Hf), cesium (Cs), europium (Eu), and samarium (Sm) show variations, with notable concentrations in all plants.
Tantalum (Ta) and terbium (Tb) are only reported in Rosemary. Strontium (Sr) and aluminum (Al) are present in all three plants, with varying levels, and zirconium (Zr) is reported only in Laurel.
This detailed elemental analysis provides a comprehensive understanding of the distribution of essential and non-essential elements in these plants, highlighting the variability and potential nutritional and toxicological implications [74] .

Despite the comprehensive analysis, some elements were not detectable using the k_0-NAA technique, due to the detection limit. The table below shows some elements and their detection limit.

Table 3.5: Elements Vs detection limit

Element	As	Cd	Cu	Hg	Se
Detection Limit (mg/kg)	0.3	3	7	3	4

To accurately quantify these elements, alternative methods such as Prompt Gamma Neutron Activation Analysis (PGNAA) (for Cd, Cu) and X-Ray Fluorescence (XRF) , Radiochemical Neutron Activation Analysis (RNAA) (for Ce, Hg, As) would be required.

The summarized results in the table are further illustrated in the following histograms, which provide a visual representation of the concentrations of EE and NEE found in the laurel, pistacia, and rosemary samples. These histograms offer a clear comparison of the elemental composition across the different plant species.

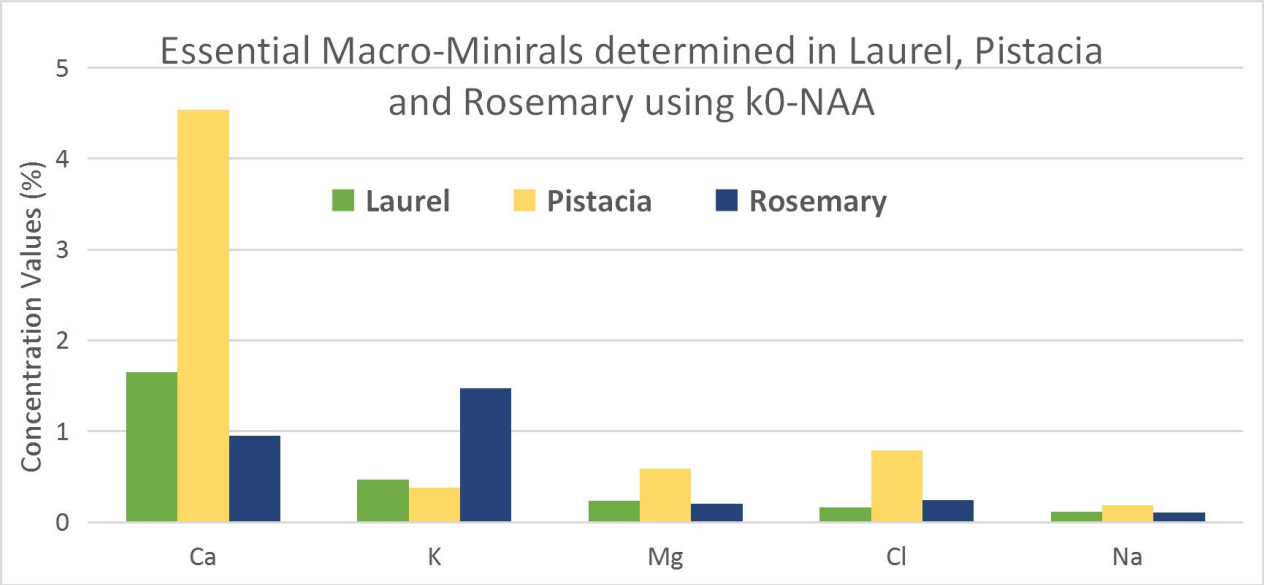

Figure 3.11: Key macro-minerals identified in laurel, pistacia, and rosemary through k_0-NAA analysis

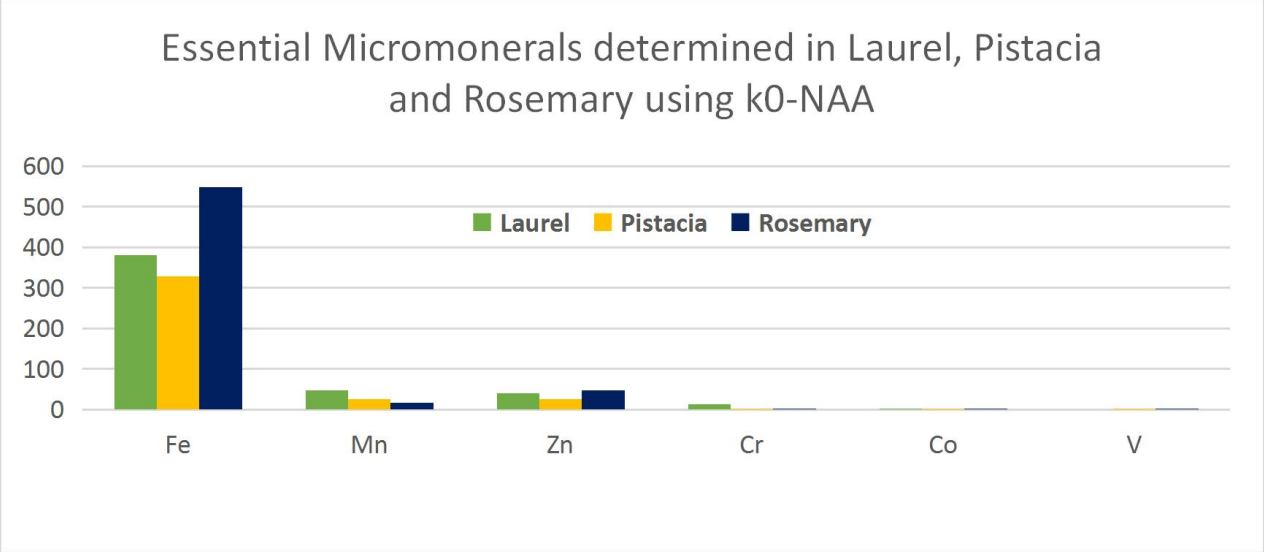

Figure 3.12: Key micro-minerals identified in laurel, pistacia, and rosemary through k_0-NAA analysis

The histograms and illustrate the concentrations of essential macro and micro-minerals in laurel, pistacia, and rosemary. Pistacia shows the highest levels of calcium (4.54%), magnesium (0.589%), and chlorine (0.79%) among the macro-minerals, while rosemary leads in potassium(1.47%). Sodium levels are relatively low across all three plants (0.107-0.19%), with pistacia having the highest concentration (0.19%). For the micro-minerals, rosemary exhibits the highest concentrations of iron (548 mg/kg), zinc (47 mg/kg), cobalt (0.297 mg/kg), and

vanadium (0.62 mg/kg). Laurel is richest in manganese (48.3 mg/kg) and chromium (13.8 mg/kg), while pistacia has moderate levels of most micro-minerals (0.219 - 328 mg/kg). These histograms highlight the nutritional diversity among these medicinal plants, emphasizing pistacia's higher macro-mineral content and rosemary's abundance in certain micro-minerals.

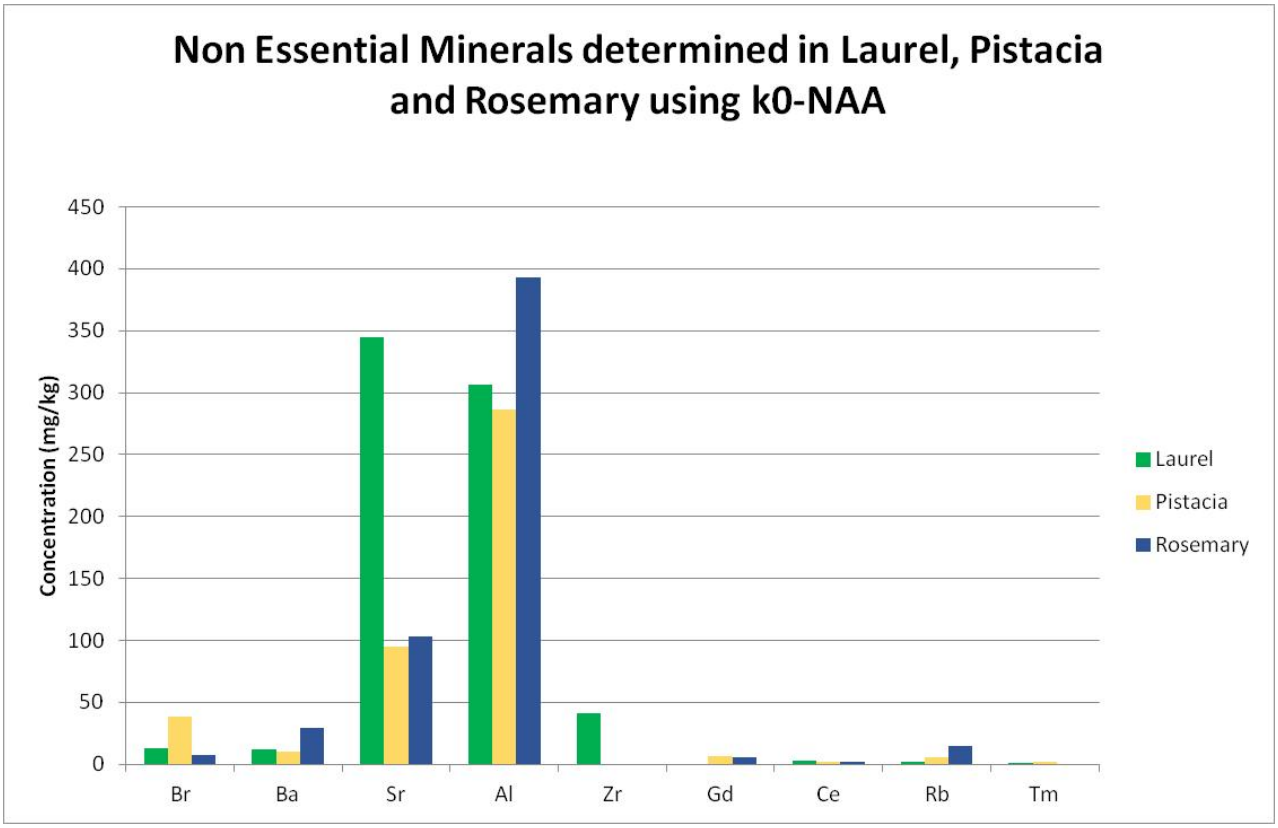

Figure 3.13: Distribution of non essential-minerals (micro) determined in studied plants

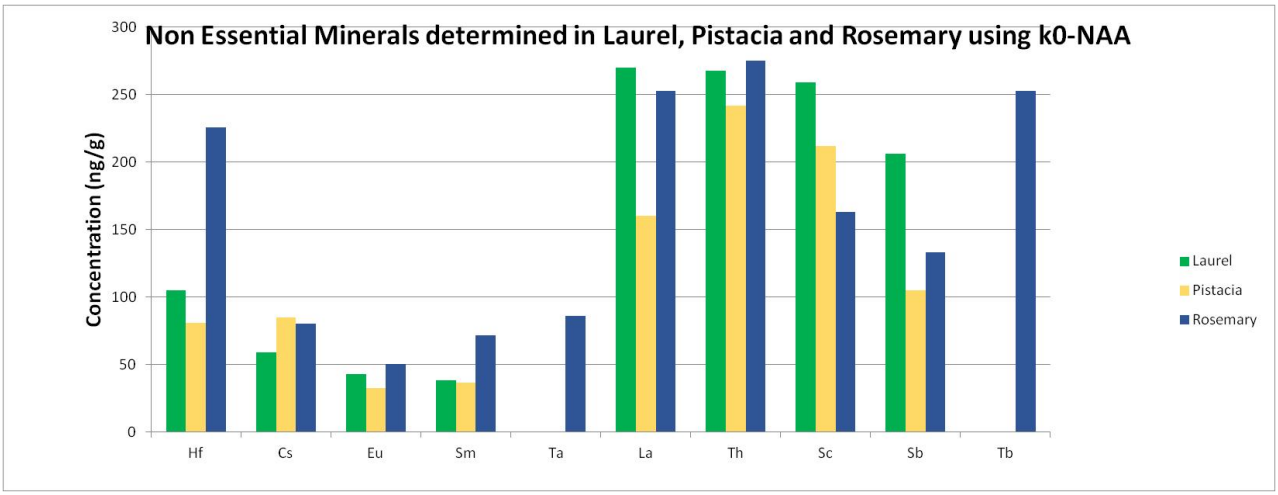

Figure 3.14: Distribution of non essential-minerals (nano) determined in studied plants

The histograms illustrate the concentration of NEE in Laurel, Pistacia, and Rosemary determined using k0-NAA. In the first histogram, Bromine (Br) concentrations are highest in Pistacia (40 mg/kg), followed by Rosemary (30 mg/kg) and Laurel (20 mg/kg), indicating different bromine absorption capacities among the plants. Strontium (Sr) shows significant concentrations, particularly high in Laurel (340 mg/kg) and Pistacia (320 mg/kg), while Aluminum (Al) is notably higher in Rosemary (400 mg/kg) compared to Laurel (300 mg/kg) and Pistacia (250 mg/kg), suggesting differences in soil or environmental aluminum availability. Zirconium (Zr) is marginally higher in Pistacia (40 mg/kg), and Gadolinium (Gd), Cerium (Ce), Rubidium (Rb), and Thulium (Tm) are present in minimal concentrations across all plants, ranging from 0 to 10 mg/kg, indicating low environmental presence or uptake.

The second histogram shows that Hafnium (Hf) is highest in Rosemary (250 ng/g), followed by Pistacia (200 ng/g) and Laurel (150 ng/g), suggesting Rosemary's higher affinity for accumulating hafnium. Cesium (Cs) concentrations are similar in Laurel and Pistacia (100 ng/g), higher than in Rosemary (60 ng/g). Europium (Eu) and Samarium (Sm) are present in low concentrations across all plants, with Eu ranging from 30 to 50 ng/g and Sm from 20 to 40 ng/g, showing slight variations. Tantalum (Ta) concentrations are low, with Rosemary (40 ng/g) having a slightly higher amount than Pistacia and Laurel (30 ng/g each). Lanthanum (La) and Thorium (Th) are high in all plants, with Laurel (250 ng/g each) showing the highest levels, followed by Pistacia and Rosemary (200 ng/g each), indicating significant soil presence. Scandium (Sc) is notably high in Laurel and Pistacia (150 ng/g each), with lower levels in Rosemary (100 ng/g). Antimony (Sb) has moderate concentrations, highest in Pistacia (120 ng/g). Terbium (Tb) concentrations are high in all plants, with Rosemary (250 ng/g) showing the highest levels, followed by Pistacia and Laurel (200 ng/g each).

Overall, the histograms highlight significant variability in NEE concentrations across the three plants, attributed to factors like soil composition, environmental conditions, and specific plant uptake mechanisms. Elements such as Aluminum and Hafnium show notable differences, suggesting specific environmental conditions or inherent differences in mineral absorption, providing insights into the nutritional and ecological characteristics of these plants.

3.3 Overall Essential Elements in Plants of Interest

After treating every element separatly we have The histogram (Figure 3.15) displays the total content of essential minerals in Pistacia, Laurel, and Rosemary, expressed as a percentage. Pistacia shows the highest overall concentration of essential minerals, significantly surpassing

Laurel and Rosemary. Calcium (Ca) is the most abundant mineral in all three plants (0.95-1.653%), with Pistacia having the highest content, followed by Laurel and Rosemary.
Potassium (K) and Magnesium (Mg) also contribute substantially to the mineral content, with Potassium being notably higher in Rosemary (1.47%) than in Pistacia and Laurel. Microminerals such as Iron (Fe), Manganese (Mn), and Zinc (Zn) are present in smaller amounts (16.9-548 mg/kg)
Iron is most abundant in Rosemary (548 mg/kg), followed by Laurel and Pistacia. Zinc content is comparable across the three plants, with Laurel having slightly higher levels (41.2 mg/kg). Cobalt (Co) and Vanadium (V) are present in trace amounts, with Pistacia having a slight advantage in Vanadium content (0.37mg/kg). The differences in mineral content among the plants can be attributed to various factors including soil composition, plant uptake mechanisms, and environmental conditions. Pistacia's higher overall mineral content might be due to its more efficient nutrient uptake and accumulation processes. Rosemary's higher Potassium content suggests it might be more effective at absorbing this particular mineral from the soil.

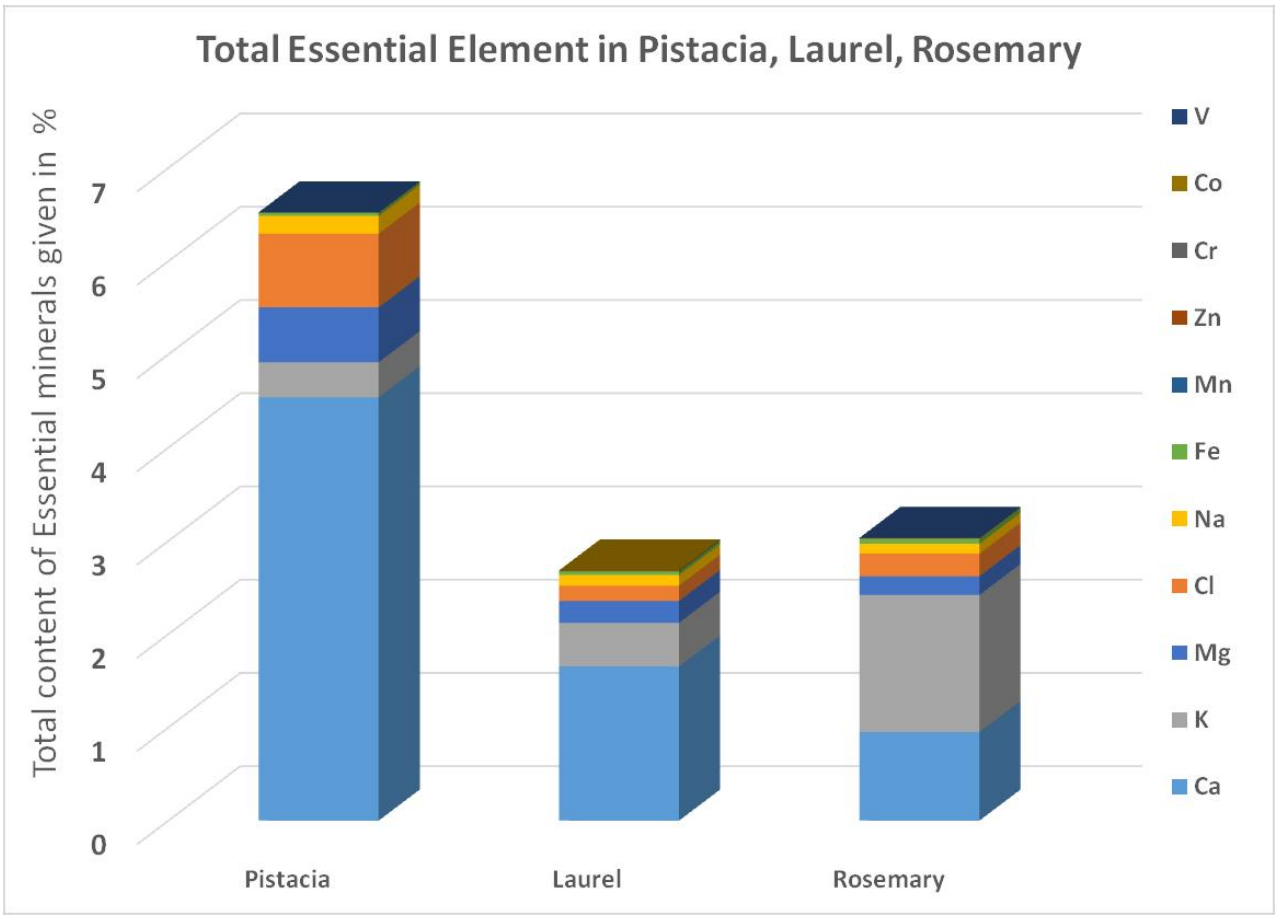

Figure 3.15: Overall essential elements in pistacia, laurel, and rosemary

Laurel shows a balanced mineral content, which might indicate moderate nutrient uptake efficiency. These variations highlight the plants' differing abilities to absorb and accumulate essential minerals from their environment.

3.4 Comparison With Litterature

By juxtaposing our data with that obtained from various regions (Morocco, Turkey, Pakistan, south algeria), we aim to highlight both the consistency and variability in the outcomes of elemental analysis. This comparison will provide deeper insights into the global patterns and potential factors influencing the observed results, thus enriching the overall understanding of the topic. The table 3.6 summarizing these comparative findings.

The table presents a comparative analysis of elemental concentrations in plants from different regions, including our current work, Morocco, Pakistan, Turkey, and South Algeria. The elements measured range from essential nutrients like Calcium (Ca), Potassium (K), and Magnesium (Mg) to trace elements and potential contaminants.
In our study, Calcium concentrations ranged from 9500 to 16530 mg/kg, which is higher compared to Morocco (13800 mg/kg) and Turkey (10899 mg/kg), and Pakistan 10500 mg/kg. Potassium showed significant variability, with our work reporting 3760 to 14700 mg/kg, whereas Morocco had 11300 mg/kg, and Turkey and South Algeria reported 9356 mg/kg and 6665.92 mg/kg, respectively. Magnesium levels in our samples ($2010 - 5890$ mg/kg) were significantly higher than in Turkey (91 mg/kg) but comparable to Pakistan (2700 mg/kg).
For Sodium (Na), our study found levels ranging from 1140 to 2010 mg/kg, higher than Morocco (461.4 mg/kg) and South Algeria (317 mg/kg). Iron (Fe) concentrations were also higher in our work ($328 - 548$ mg/kg) compared to Morocco (201.4 mg/kg) and South Algeria (162.12 mg/kg), but comparable to Turkey (547 mg/kg). Manganese (Mn) was found in the range of $16.9 - 48.3$ mg/kg in our study, which is higher than Turkey (15.59 mg/kg) and South Algeria (10.94 mg/kg) but lower than Morocco (78.81 mg/kg).
Zinc (Zn) concentrations in our study ($26.8 - 47$ mg/kg) were higher than Morocco (19.58 mg/kg) and Turkey ($0.37 mg/kg$), while Chromium (Cr) levels ($1.41 - 13.8$ mg/kg) were higher than Morocco (5.01 mg/kg) and South Algeria (1.47 mg/kg), but comparable to Turkey (8.93 mg/kg).
Cobalt (Co) levels in our study ($0.219 - 0.297$ mg/kg) were lower than Morocco and Turkey (0.59 mg/kg) but higher than South Algeria (1.141 mg/kg).
Variations in elemental concentrations can be attributed to differences in soil composition, agricultural practices, and environmental factors specific to each region. For instance, high

levels of Calcium and Magnesium in our study could be due to the type of soil and fertilizers used, whereas lower levels of some elements in other regions might indicate different soil chemistry or less use of specific fertilizers.

Table 3.6: Comparison of Elemental Analysis Results in (mg/kg)

Element	**This Work**	**Morocco [75]**	**Pakistan [76]**	**Turkey [77]**	**Algeria [78]**
Ca	9500 - 16530	13800	10500	10899	7858.92
K	3760 - 14700	11300	21500	9356	6665.92
Mg	2010 - 5890	1300	2700	91	1605.97
Cl	1640 - 7900	-	1900	-	-
Na	1140 - 2010	461.4	-	461.4	317
Fe	328 - 548	201.4	-	547	162.12
Mn	16.9 - 48.3	78.81	-	15.59	10.94
Zn	26.8 - 47	19.58	-	0.37	32.88
Cr	1.41 - 13.8	5.01	-	8.93	1.47
Co	0.219 - 0.297	0.59	-	0.59	1.141
V	0.37 - 0.62	24.39	-	-	-
Br	7.58 - 38.04	-	-	-	9.16
Ba	10.1 - 29	-	-	95.5	-
Gd	5.7 - 6.7	-	-	-	-
Ce	1.57 - 3	-	-	-	1.126
Rb	1.95 - 14.8	-	-	-	5.51
Tm	1.05 - 1.85	-	-	-	-
La	0.16 - 0.27	14.09	-	-	0.61
Th	0.242 - 0.275	-	-	-	-
Sc	0.163 - 0.259	-	-	-	0.112
Sb	0.105 - 0.206	-	-	-	0.064
Hf	0.081 - 0.226	-	-	-	-
Cs	0.059 - 0.085	-	-	-	0.114
Eu	0.032 - 0.05	-	-	-	-
Sm	0.036 - 0.071	-	-	-	0.303
Ta	0.086	-	-	-	-
Tb	0.253	-	-	-	-
Sr	95 - 345	-	-	-	0.23
Al	286 - 393	287.8	1400	486	-
Zr	41	-	-	-	-

Regarding toxic elements, Vanadium (V) and Chromium (Cr) are noteworthy. In our work, Vanadium was found at $0.37 - 0.62$ mg/kg, significantly lower than Morocco (24.39 mg/kg). Chromium, a known carcinogen, was present in our samples at $1.41 - 13.8$ mg/kg, higher than Morocco (5.01 mg/kg) and comparable to Turkey (8.93 mg/kg). The presence of these elements at such levels calls for regular monitoring to ensure they remain within safe limits for consumption. Reducing the use of contaminated fertilizers and adopting practices that limit soil contamination can help mitigate the risks associated with these toxic elements.

3.5 Recommended Dietary Allowance (RDA)

The RDA values provide recommended daily intakes tailored for both males and females, ensuring adequate nutrition. By juxtaposing these standards with our elemental analysis results, we aim to assess the adequacy of elemental intake levels in relation to optimal health recommendations.

The next table details the RDA (Recommended Dietary Intake) values and compares them with the elemental concentrations detected in our study. This comparison will help elucidate whether observed levels meet, exceed, or fall below recommended dietary allowances, offering insights into potential nutritional imbalances or adequacies.

Table 3.7: Comparison of various mineral contents in Laurel, Pistacia, and Rosemary with their Recommended Daily Allowances (RDA) and Dietary Intakes (DI) for both females (F) and males (M) in (mg/day).

	Ca	K	Mg	Na	Mn	Fe	Zn	Cr	V
Plants	81.85	73.5	29.45	10.05	0.241	2.47	4.7	0.001175	0.0031
RDA (F)*	1000	4700	320	1500	1.8	18	8	0.025	8
RDA (M)*	1000	4700	420	1500	2.3	8	11	0.035	10
DI (mg/day)	165-265	275-473	176-253	12.4-18.5	1.7-6.8	8.4-11.7	2.2-7.4	0.0002-0.0023	10
Limit	2500	-	350	-	11	45	40	-	>10

DI : Daily Intake

F* : Female

M* : Male

The table presents a comparison between the daily intake of various minerals from consuming the medicinal plants and the Recommended Dietary Allowances (RDA) for females and males as established by the Food and Agriculture Organization (FAO). Calcium (Ca) intake from the plants is 81.85 mg/day, significantly lower than the RDA of 1000 mg/day for both males and females, and also well within the upper limit of 2500 mg/day. Potassium (K) intake is 73.5 mg/day, also considerably below the RDA of 4700 mg/day for both genders. Magnesium (Mg) intake ranges from 29.45 mg/day, again much lower than the RDA of 320 mg/day for females and 420 mg/day for males, and below the upper limit of 350 mg/day. Sodium (Na) intake is 10.05 mg/day, far below the RDA of 1500 mg/day. Manganese (Mn) intake is 0.241 mg/day, significantly lower than the RDA of 1.8 mg/day for females and 2.3 mg/day for males, and well within the upper limit of 11 mg/day. Iron (Fe) intake from plants is 2.47 mg/day, below the RDA of 18 mg/day for females and 8mg/day for males, and below the upper limit of 45 mg/day. Zinc (Zn) intake is 4.7 mg/day, lower than the RDA of 8 mg/day for females and 11 mg/day for males, and well within the upper limit of 40 mg/day.

For chromium (Cr) and vanadium (V), which are considered toxic elements, the intake from plants is 0.001175 mg/day for Cr, significantly below the RDA of 0.025 mg/day for females and 0.035 mg/day for males. Vanadium intake is 0.0031 mg/day, while the safe intake level is suggested to be around 10 mg/day. These low intakes of Cr and V indicate minimal risk of toxicity.

To calculate the daily intake of a substance from its concentration in food, expressed in mg/kg, it is essential to determine the daily consumption of that food in kilograms. The daily intake in milligrams is then obtained by multiplying the concentration by the daily intake amount. The formula for this calculation is:

$$DI = C * DI_f$$

Where :
DI : Daily Intake (mg/kg)
C : Concentration
DI_f : Daily Intake of Food (kg/day)
This approach allows for an accurate translation of the nutrient or element concentration in foods into a quantifiable daily intake, providing a clear understanding of dietary intake based on consumption patterns.

3.6 Conslusion

This chapter utilized the k_0-Neutron Activation Analysis (k_0-NAA) technique to analyze three medicinal plants: Pistacia lentiscus, Rosmarinus officinalis, and Laurus nobilis. Through experiments involving short irradiation in a pneumatic system and long/medium irradiation in a vertical canal, we identified and quantified 30 elements, including essential minerals like Ca, K, Mg, and trace elements such as Fe, Zn, and V.

Pistacia lentiscus exhibited the highest overall concentration of essential minerals, with Calcium (Ca) being the most abundant element across all plants (0.95-1.653%). Rosmarinus officinalis stood out with notably higher Potassium (K) levels (1.47%) compared to the other plants. Iron (Fe) was most abundant in Rosmarinus officinalis (548 mg/kg), while Pistacia lentiscus showed a slight advantage in Vanadium (V) content (0.37 mg/kg).

Comparisons with recommended daily allowances (RDA) from the Food and Agriculture Organization (FAO) indicated that all elemental concentrations were within safe limits. The k_0-NAA technique demonstrated its efficacy in providing detailed elemental profiles, essential for assessing the nutritional and therapeutic potential of these medicinal plants. Its ability to accurately quantify multiple elements simultaneously without chemical separation underscores its significance in advancing nutritional and pharmacological research.

General conclusion

This work aimed to conduct a comparative study of essential and toxic elements in medicinal plants —Laurel (Laurus nobilis), Pistacia (Pistacia lentiscus), and Rosemary (Rosmarinus officinalis)— using the k_0-NAA technique. The primary research problem focused on quantifying and comparing the concentrations of these elements to understand their potential health benefits and risks. This work allowed us to identify 30 elements (Ca, K, Mg, Cl, Na, Fe, Mn, Zn, Cr, Co, V, Br, Ba, Gd, Ce, Rb, Tm, La, Th, Sc, Sb, Hf, Cs, Eu, Sm, Ta, Tb, Sr, Al, Zr), with Pistacia lentiscus being the richest in nutrients.

We conducted two experiments: short irradiation in a pneumatic system and medium to long irradiation in a vertical channel. The results obtained were meticulously compared with data from existing literature (Morocco, Turkey, Pakistan, and other regions of Algeria), highlighting the unique elemental compositions of these medicinal plants. Through this comparative analysis, we gained valuable insights into the nutritional and therapeutic attributes of these plants.

Furthermore, the results were rigorously validated against standard reference analyses (NIST-1573a and GSV4), ensuring their precision and accuracy. This meticulous verification process bolstered the credibility of our findings, affirming the reliability of the identified elemental compositions. By adhering to established standards, we confidently assert the exactness of our results, providing a robust foundation for further research and practical applications. This assurance of accuracy strengthens the significance of our study, elevating its contribution to the scientific understanding of these medicinal plants and their potential health implications. This work serves as a reliable resource for researchers, students, and practitioners, enhancing understanding and application in diverse fields.

The study revealed significant variations in the concentrations of both essential macrominerals and microminerals, as well as non-essential elements across the three plants. For instance, Laurel exhibited high levels of calcium (1.653%), while Rosemary showed substantial amounts of potassium (1.47%) and the highest concentration of iron (548 mg/kg). Manganese concentrations were highest in Laurel (48.3 mg/kg), followed by Pistacia (25.6 mg/kg), and lowest in Rosemary (16.9 mg/kg).

These findings contribute to the existing body of knowledge by providing precise elemental compositions of these medicinal plants, highlighting their nutritional and toxicological profiles. Practically, this information is crucial for healthcare professionals and herbal practitioners to optimize the use of these plants in treatments, ensuring their benefits while minimizing potential risks. It also serves as a guideline for policymakers in regulating the use of these plants.
The study successfully met its objectives by using the k_0-NAA technique to detect and quantify the elements in the medicinal plants, validating the method's efficacy in this context by calculating Z-score and U-score. The hypotheses regarding the variation in elemental concentrations among the plants were supported by the findings.
Additionally, we worked with the Recommended Daily Allowance (RDA) to assess the nutritional contributions of these plants. Future studies should explore a wider range of medicinal plants and consider the influence of environmental factors on elemental concentrations. Longitudinal studies could also assess the consistency of these elements over different growth stages and conditions.
This research underscores the importance of understanding the elemental composition of medicinal plants, by providing a scientific basis for their use in traditional and modern medicine.
In conclusion, this study offers valuable insights into the essential and toxic elements present in Laurel, Pistacia, and Rosemary using the k_0-NAA technique. These findings pave the way for safer and more effective utilization of medicinal plants, ensuring their benefits while mitigating risks.

Bibliography

[1] Egle Milia, Simonetta Maria Bullitta, Giorgio Mastandrea, Barbora Szotáková, Aurélie Schoubben, Lenka Langhansová, Marina Quartu, Antonella Bortone, and Sigrun Eick. Leaves and fruits preparations of pistacia lentiscus l.: A review on the ethnopharmacological uses and implications in inflammation and infection. *Antibiotics*, 10:425, 4 2021.

[2] Mohannad G AL-Saghir and Duncan M Porter. Taxonomic revision of the genus pistacia l.(anacardiaceae). *American Journal of plant sciences*, 3(1):12, 2012.

[3] Antonello Paparella, Bhagwat Nawade, Liora Shaltiel-Harpaz, and Mwafaq Ibdah. A review of the botany, volatile composition, biochemical and molecular aspects, and traditional uses of laurus nobilis, 5 2022.

[4] Tran Tham Thuy Do, Bao Ngoc Vu, Thi Binh Hoang, et al. Effect of enzyme-assisted extraction on yield, composition, and antimicrobial activity of essential oils from rosmarinus officinalis l. grown in lam dong province, viet nam. *CTU Journal of Innovation and Sustainable Development*, 14(3):65–71, 2022.

[5] P Pablo Ferrer-Gallego, Raul Ferrer-Gallego, Roberto Rosello, Juan B Peris, Alberto Guillen, Jose Gomez, and Emilio Laguna. A new subspecies of rosmarinus officinalis (lamiaceae) from the eastern sector of the iberian peninsula. *Phytotaxa*, 172(2):61–70, 2014.

[6] International Atomic Energy Agency. Gamma and alpha spectrometry for workplace monitoring content objectives need for spectrometry method of analysis introduction to alpha and gamma spectrometry.

[7] Belkessa Kahina. Mesure de flux de neutrons pour une source ra-be par la méthode d'analyse par activation neutronique. 2018.

[8] K Buchtela. Gamma-ray spectrometry.

[9] Genie 2k Spectroscopy Software. Customization tools and operation manuals.

[10] Google Maps. Location map of blida, 2024. Accessed: 2024-04-15.

[11] Samir Begaa, Mohammed Messaoudi, Abdelkader Ouanezar, Lylia Hamidatou, and Abderrahim Malki. Chemical elements of algerian mentha spicata l. used in the treatment of digestive system disorders by employing instrumental neutron activation analysis technique. *Journal of Radioanalytical and Nuclear Chemistry*, 317(2):1107–1112, 2018.

[12] Lylia Hamidatou, Hocine Slamene, and Lahcen Si Mohamed. Major, minor and trace elements in four kinds of cement powder using inaa and k 0-standardization methods. *Journal of Radioanalytical and nuclear chemistry*, 304:717–725, 2015.

[13] Lylia Hamidatou-Alghem, Hocine Slamene, and Kamel Djebli. Performance evaluation of the laboratory applying k0-naa at es-salam research reactor during 2021–2022. *Journal of Radioanalytical and Nuclear Chemistry*, 332(8):3515–3521, 2023.

[14] L Hamidatou, H Slamene, T Akhal, B Zouranen, S Begaa, M Messaoudi, M Touiza, S Laour, and M Salhi. Algerian neutron activation analysis: Laboratory of crnb: Recent and future action plan. Technical report, 2017.

[15] Lylia Hamidatou, Hocine Slamene, Tarik Akhal, Samir Begaa, Mohammed Messaoudi, and Zouranen Boussaad. Naa algerian laboratory evaluation processed by wepal and iaea during 2011-2012. *Journal of Analytical Sciences, Methods and Instrumentation*, 2013, 2013.

[16] Lylia Hamidatou and Houcine Benkharfia. Experimental and mcnp calculations of neutron flux parameters in irradiation channel at es-salam reactor. *Journal of Radioanalytical and Nuclear Chemistry*, 287:971–975, 2011.

[17] Bouzid Nedjimi. Measurement of selenium in two algerian chenopods (atriplex canescens (pursh.) nutt. and suaeda fruticosa (linn.) forssk). *Measurement*, 129:256–259, 2018.

[18] Lylia Hamidatou, Fahd Arbaoui, Mohamed Nadir Boucherit, and Hocine Slamene. Determination of chemical elements in two algerian bentonites by k 0-naa and wdxrf techniques. *Journal of Radioanalytical and Nuclear Chemistry*, 332(3):573–580, 2023.

[19] L Hamidatou, H Slamene, B Dbacha, M Aït-Ziane, A Badreddine, N Benaskeur, H Benkharfia, M Alliti, K Attari, M Hachouf, et al. Experimental determination and simulation of neutron and gamma flux parameters in horizontal channel for prompt gamma neutron activation analysis implementation at es-salam research reactor. *Applied Radiation and Isotopes*, 174:109759, 2021.

[20] Mohammed Messaoudi, Samir Begaa, Lylia Hamidatou, and M'hamed Salhi. Determination of selenium in roasted beans coffee samples consumed in algeria by radiochemical neutron activation analysis method. *Radiochimica Acta*, 106(2):141–146, 2018.

[21] S Khaled, S Belaid, M Mouzai, L Alghem, A Ararem, and B Zouranen. Development and application of the cyclic delayed neutron counting technique at es-salam research reactor. *Physical & chemical news*, (45):39–43, 2009.

[22] L. Alghem, M. Ramdhane, S. Khaled, and T. Akhal. The development and application of k0-standardization method of neutron activation analysis at es-salam research reactor. *Nuclear Instruments and Methods in Physics Research Section A: Accelerators, Spectrometers, Detectors and Associated Equipment*, 556(1):386–390, 2006.

[23] S Khaled, M Mouzai, A Ararem, L Hamidatou, and B Zouranen. Elemental analysis of traditional medicinal seeds by instrumental neutron activation analysis. *Journal of radioanalytical and nuclear chemistry*, 281(1):87–90, 2009.

[24] L. Hamidatou, H. Slamene, and K. Djebli. Internal and external quality control procedures applied for k0-neutron activation analysis laboratory using Es-Salam research reactor. *AIP Conference Proceedings*, 1994(1):040005, 08 2018.

[25] Chabha Sehaki, Nathalie Jullian, Fadila Ayati, Farida Fernane, and Eric Gontier. A review of pistacia lentiscus polyphenols: Chemical diversity and pharmacological activities. *Plants*, 12:279, 1 2023.

[26] Egle Patrizia Milia, Luigi Sardellitti, and Sigrun Eick. Antimicrobial efficiency of pistacia lentiscus l. derivates against oral biofilm-associated diseases—a narrative review, 6 2023.

[27] S Landau, H Muklada, A Marcovics, and H Azaizeh. Traditional uses of pistacia lentiscus in veterinary and human medicine.

[28] Moncef Beldi, Hayette Merzougui, and Amel Lazli. Etude ethnobotanique du pistachier lentisque pistacia lentiscus l. dans la wilaya d'el tarf (nord-est algérien) - ethnobotanical study of pistacia lentiscus l. in el tarf region (northeastern algeria). *Ethnobotany Research and Applications*, 21, 2 2021.

[29] Miguel Verdú and Patricio García-Fayos. The effect of deceptive fruits on predispersal seed predation by birds in pistacia lentiscus. *Plant Ecology*, 2000.

[30] Kaissa Boudieb, Sabrina Ait Slimane-Ait Kaki, and Hayet Amellal-Chibane. Traditional uses, phytochemical study and morphological characterization of pistacia lentiscus l. fruits from three areas of northern algeria. *Journal of Applied Biosciences*, 135:13788, 5 2019.

[31] A. Golan-Goldhirsh, O. Barazani, Z. S. Wang, D. K. Khadka, J. A. Saunders, V. Kostiukovsky, and L. J. Rowland. Genetic relationships among mediterranean pistacia species evaluated by rapd and aflp markers. *Plant Systematics and Evolution*, 246:9–18, 4 2004.

[32] Christodoulos Anagnostou, Stavros Beteinakis, Anastasia Papachristodoulou, Vasiliki K. Pachi, Mariangela Dionysopoulou, Sofia Dimou, George Diallinas, Leandros A. Skaltsounis, and Maria Halabalaki. Phytochemical investigation of pistacia lentiscus l. var. chia leaves: A byproduct with antimicrobial potential. *Fitoterapia*, 170, 10 2023.

[33] O Z Barazani, Nativ Dudai, and Avi Golan-Goldhirsh. Comparison of mediterranean pistacia lentiscus genotypes by random amplified polymorphic dna, chemical, and morphological analyses 1940 barazani, dudai, and golan-goldhirsh, 2003.

[34] Biljana Kaurinovic, Mira Popovic, and Sanja Vlaisavljevic. In vitro and in vivo effects of laurus nobilis l. leaf extracts. *Molecules*, 15:3378–3390, 5 2010.

[35] Kristina Pilipović, Renata Jurišić Grubešić, Petra Dolenec, Natalia Kučić, Lea Juretić, and Jasenka Mršić-Pelčić. Plant-based antioxidants for prevention and treatment of neurodegenerative diseases: Phytotherapeutic potential of laurus nobilis, aronia melanocarpa, and celastrol, 3 2023.

[36] Ouibrahim A, Tlili Ait kaki Y, Bennadja S, Amrouni S, G Djahoudi A, and R Djebar M. Evaluation of antibacterial activity of laurus nobilis l., rosmarinus officinalis l. and ocimum basilicum l. from northeast of algeria. *African Journal of Microbiology Research*, 7, 10 2013.

[37] Ramling Patrakar, Meera Mansuriya, and Priyanka Patil. International journal of pharmaceutical and chemical sciences phytochemical and pharmacological review on laurus nobilis.

[38] H. Marzouki, A. Piras, K. Bel Haj Salah, H. Medini, T. Pivetta, S. Bouzid, B. Marongiu, and D. Falconieri. Essential oil composition and variability of laurus nobilis l. growing in tunisia, comparison and chemometric investigation of different plant organs. *Natural Product Research*, 23:343–354, 2009.

[39] Jouda Mediouni Ben Jemâa, Nesrine Tersim, Karima Taleb Toudert, and Mohamed Larbi Khouja. Insecticidal activities of essential oils from leaves of laurus nobilis l. from tunisia, algeria and morocco, and comparative chemical composition. *Journal of Stored Products Research*, 48:97–104, 1 2012.

[40] Kodoth Prabhakaran Nair. *Herbal and Acidulant Tree Spices: Their Global Commercial Potential*. Springer International Publishing, 1 2022.

[41] Jonatas Rafael De Oliveira, Samira Esteves Afonso Camargo, and Luciane Dias De Oliveira. Rosmarinus officinalis l.(rosemary) as therapeutic and prophylactic agent. *Journal of biomedical science*, 26(1):5, 2019.

[42] Dejene Tadesse Banjaw, Habtamu Gudisa Megersa, Damtew Abewoy, and Dadi Tolessa Lema. Rosemary recent classification, plant characteristics, economic parts, marketing, uses, chemical composition, and cultivation.

[43] K Haile Asressu and T Kebede Tesema. Chemical and antimicrobial investigations on essential oil of rosmarinus officinalis leaves grown in ethiopia and comparison with other countries. *Journal of Applied Pharmacy*, 6(2):132–142, 2014.

[44] Guido Flamini, Pier Luigi Cioni, Ivano Morelli, Mario Macchia, and Lucia Ceccarini. Main agronomic- productive characteristics of two ecotypes of rosmarinus officinalis l. and chemical composition of their essential oils. *Journal of Agricultural and Food Chemistry*, 50(12):3512–3517, 2002.

[45] Sota Fujii, Ken-ichi Kubo, and Seiji Takayama. Non-self-and self-recognition models in plant self-incompatibility. *Nature plants*, 2(9):1–9, 2016.

[46] S Santoyo, S Cavero, L Jaime, E Ibanez, FJ Senorans, and G Reglero. Chemical composition and antimicrobial activity of rosmarinus officinalis l. essential oil obtained via supercritical fluid extraction. *Journal of food protection*, 68(4):790–795, 2005.

[47] Abayneh Kassahun and Gezu Feleke. Proximate analysis, physicochemical properties and chemical constituent's characterization of rosemarinus officinalis oil. *Natural Volatiles and Essential Oils*, 6(2):20–24, 2019.

[48] EL Saad, Salem S Salem, Amr Fouda, Mohamed A Awad, Mamdouh S El-Gamal, and Abdullah M Abdo. New approach for antimicrobial activity and bio-control of various pathogens by biosynthesized copper nanoparticles using endophytic actinomycetes. *Journal of Radiation Research and Applied Sciences*, 11(3):262–270, 2018.

[49] Attilio Anzano, Bruna de Falco, Laura Grauso, Riccardo Motti, and Virginia Lanzotti. Laurel, laurus nobilis l.: a review of its botany, traditional uses, phytochemistry and pharmacology, 4 2022.

[50] Asma El Zerey-Belaskri, Nabila Belyagoubi-Benhammou, and Hachemi Benhassaini. From traditional knowledge to modern formulation: potential and prospects of pistacia atlantica desf. essential and fixed oils uses in cosmetics. *Cosmetics*, 9(6):109, 2022.

[51] Menno Blaauw, Giancarlo D'Agostino, Marco di Luzio, Ho Manh Dung, Radojko Jacimovic, Mauro Da Silva Dias, Renato Semmler, Robbert van Sluijs, and Nuno Pessoa Barradas. The 2021 iaea software intercomparison for k0-inaa. *Journal of Radioanalytical and Nuclear Chemistry*, 332(8):3387–3400, 2023.

[52] R Van Sluijs and DAWJ Bossus. Optimized data evaluation for k 0-based naa. *Journal of radioanalytical and nuclear chemistry*, 239(3):601–603, 1999.

[53] Matthias Rossbach and Menno Blaauw. Progress in the k0-iaea program. *Nuclear Instruments and Methods in Physics Research Section A: Accelerators, Spectrometers, Detectors and Associated Equipment*, 564(2):698–701, 2006.

[54] L Alghem Hamidatou and M Ramdhane. Characterization of neutron spectrum at essalam research reactor using høgdahl convention and westcott formalism for the k 0-based neutron activation analysis. *Journal of Radioanalytical and Nuclear Chemistry*, 278:627–630, 2008.

[55] Ho Manh Dung and Pham Duy Hien. The application and development of k 0-standardization method of neutron activation analysis at dalat research reactor. *Journal of Radioanalytical and Nuclear Chemistry*, 257:643–647, 2003.

[56] Andrej Trkov and Vladimir Radulović. Nuclear reactions and physical models for neutron activation analysis. *Journal of Radioanalytical and Nuclear Chemistry*, 304(2):763–778, 2015.

[57] Robert R Greenberg, Peter Bode, and Elisabete A De Nadai Fernandes. Neutron activation analysis: A primary method of measurement. *Spectrochimica acta part B: atomic spectroscopy*, 66(3-4):193–241, 2011.

[58] LH ALGHEM. Advanced technologies and applications of neutron activation analysis, 2019.

[59] H Bounouira, K Embarch, H Amsil, M Bounakhla, S Foudeil, F Benyaich, M Haddad, F Said, et al. Study of heavy metal assessment in the gharb plain along sebou river (morocco) using k0-naa method at the moroccan triga mark ii research reactor. *Annals of Agrarian Science*, 16(4):376–388, 2018.

[60] Jasna Humerovic, Tidza Muhic-Sarac, Mustafa Memic, Sabina Zero, and Alisa Selovic. Multielement and rare earth element composition of the soil and lichen from sarajevo, bosnia and herzegovina. *Ekoloji*, 24(97):36, 2015.

[61] AR Yavar, S Sarmani, AK Wood, SM Fadzil, Z Masood, and KS Khoo. Neutron flux parameters for k0-naa method at the malaysian nuclear agency research reactor after core reconfiguration. *Radiation Measurements*, 46(2):219–223, 2011.

[62] A El Abd and M Mostafa. Determination of the impurities concentration in tungsten, molybdenum, tin, and tellurium targets using neutron activation analysis techniques. *Yaderna Fyizika ta Energetika*, 10(4):437–445, 2009.

[63] T Doumaz, L Hamidatou, B Beladel, H Slamene, S Begaa, M Messaoudi, M Arezki, S Amalou, M Benmahdioub, and MEA Benamar. Major and trace elements determination in algerian alzheimer patients by k0-naa method. *Journal of Radioanalytical and Nuclear Chemistry*, 309(1):229–234, 2016.

[64] Frans De Corte, A De Wispelaere, R Van Sluijs, D Bossus, A Simonits, J Kučera, J Frána, B Smodis, and R Jaćimović. The installation of kayzero-assisted naa for use in industry and environmental sanitation in three central european countries: Plans and achievements of a copernicus project. *Journal of radioanalytical and nuclear chemistry*, 215:31–37, 1997.

[65] Lylia Hamidatou, Hocine Slamene, Tarik Akhal, and Alaa Boulegane. Trace and essential elements determination in baby formulas milk by inaa and k 0-inaa techniques. *Journal of Radioanalytical and nuclear chemistry*, 301:659–666, 2014.

[66] Mauro S Dias, Vanderlei Cardoso, Marina F Koskinas, and Ione M Yamazaki. Determination of the neutron spectrum shape parameter α in k0 naa methodology using covariance analysis. *Applied Radiation and Isotopes*, 68(4-5):592–595, 2010.

[67] A. Courti, P. Bouisset, and P. Chevallier. Beta spectrometry for environmental radioactivity measurements. *Radioprotection*, 37:C1–911–C1–916, 2 2002.

[68] Mansouri rania and Zaida malak. Analyse par activation neutronique instrumentale des échantillons de phosphates : utilisation des voies de moyennes et longues périodes, 2023.

[69] Özlem Karadeniz and Sabiha Vurmaz. Experimental investigation on the photopeak efficiency of a coaxial high purity germanium detector for different geometries. *Journal of Basic and Clinical Health Sciences*, 1(1):18–22, 2017.

[70] volume=139 number=2 pages=134 year=2024 publisher=Springer Hafizoglu, journal=The European Physical Journal Plus. Efficiency and energy resolution of gamma spectrometry system with hpge detector depending on variable source-to-detector distances.

[71] et al De Corte, F. k0-based naa standardization: principles, practice and applications. *Journal of Radioanalytical and Nuclear Chemistry*, 257(3):493–500, 2003.

[72] Brahim Meftah. Outlook of nuclear energy in algeria. In *International Conference On Opportunities and Challenges for Water Cooled Reactorsin The 21St Century*, pages 1–4. IAEA Vienna, Austria, 2009.

[73] VP Kolotov and Frans De Corte. An electronic database with a compilation of k 0 and related data for naa. *Journal of radioanalytical and nuclear chemistry*, 257:501–508, 2003.

[74] National Research Council, Commission on Life Sciences, and Subcommittee on the Tenth Edition of the Recommended Dietary Allowances. Recommended dietary allowances. 1989.

[75] Amena Mrabet, Bahia Abdelfattah, Fouad El Mansouri, Ayoub Simou, and Mohamed Khaddor. Bay laurel of northern morocco: A comprehensive analysis of its phytochemical profile, mineralogical composition, and antioxidant potential. *Biophysica*, 4(2):238–255, 2024.

[76] Sulaiman, SM Shah, Sadaf, M Amin, B Gul, and M Begum. Ethnoecological, elemental, and phytochemical evaluation of five plant species of lamiaceae in peshawar, pakistan. *Scientifica*, 2020(1):2982934, 2020.

[77] Mehmet Zengin, Mehmet Musa Özcan, Ümmühan Çetin, and Sait Gezgin. Mineral contents of some aromatic plants, their growth soils and infusions. *Journal of the Science of Food and Agriculture*, 88(4):581–589, 2008.

[78] Nadjia Hamlat, Adel Benarfa, Brahim Beladel, Samir Begaa, Mohammed Messaoudi, and Aicha Hassani. Assessment of the contents of essential and potentially toxic elements in pistacia terebinthus l. and pistacia lentiscus l. by inaa technique. *Journal of Radioanalytical and Nuclear Chemistry*, 322(2):1127–1131, 2019.

[79] Miguel Verdú and Patricio García-Fayos. The effect of deceptive fruits on predispersal seed predation by birds in pistacia lentiscus. 2000.

[80] Nadjia Hamlat, Adel Benarfa, Brahim Beladel, Samir Begaa, Mohammed Messaoudi, and Aicha Hassani. Assessment of the contents of essential and potentially toxic elements in pistacia terebinthus l.and pistacia lentiscus l.by inaa technique. *Journal of Radioanalytical and Nuclear Chemistry*, 322:1127–1131, 11 2019.

[81] Glenn F. Knoll. *Radiation Detection and Measurement*. Wiley, New York, 2010.

[82] Fatma Tuğçe Gürağaç Dereli, Mert Ilhan, and Tarun Belwal. *Novel Drug Targets With Traditional Herbal Medicines: Scientific and Clinical Evidence*. Springer International Publishing, 1 2022.

[83] Francisco José González-Minero, Luis Bravo-Díaz, and Antonio Ayala-Gómez. Rosmarinus officinalis l. (rosemary): An ancient plant with uses in personal healthcare and cosmetics. *Cosmetics*, 7:77, 10 2020.

[84] IA Alnour, H Wagiran, N Ibrahim, Suhaimi Hamzah, WB Siong, and Mohd Suhaimi Elias. New approach for calibration the efficiency of hpge detectors. In *AIP conference proceedings*, volume 1584, pages 38–44. American Institute of Physics, 2014.

[85] Horst Marschner. *Marschner's Mineral Nutrition of Higher Plants*. Academic Press, 2011.

[86] Lincoln Taiz and Eduardo Zeiger. Plant physiology sinauer associates. *Inc., Publisher. Sunderland, Massachussetts*, 2006.

[87] Konrad Mengel and Ernest A Kirkby. *Principles of plant nutrition.* Number Ed. 4. 1987.

[88] Emanuel Epstein and Arnold J Bloom. *Mineral nutrition of plants: principles and perspectives*. Sinauer, 1853.

[89] Eugene V Maas and Glenn J Hoffman. Crop salt tolerance—current assessment. *Journal of the irrigation and drainage division*, 103(2):115–134, 1977.

[90] M Lou Guerinot and Ying Yi. Iron: nutritious, noxious, and not readily available. *Plant physiology*, 104(3):815, 1994.

[91] Henryk Pendias et al. Trace elements in soils and plants. 1992.

[92] Brian J Alloway. Zinc in soils and crop nutrition. 2008.

[93] Luisa MPF Amaral, Tania Moniz, André MN Silva, and Maria Rangel. Vanadium compounds with antidiabetic potential. *International Journal of Molecular Sciences*, 24(21):15675, 2023.

[94] Lylia Hamidatou, Hocine Slamene, Tarik Akhal, and Boussaad Zouranen. Concepts, instrumentation and techniques of neutron activation analysis. *Imaging and Radioanalytical Techniques in Interdisciplinary Research-Fundamentals and Cutting Edge Applications*, pages 141–178, 2013.

Abstract

This study presents a comparative analysis of essential and toxic elements in Laurus nobilis, Pistacia lentiscus, and Rosmarinus officinalis using the k_0-Neutron Activation Analysis .The technique provided high sensitivity and accuracy in quantifying elements. Detected elements include major (Ca 0.95%-1.653%, K 0.376 %-1.47%, Mg 0.201%-0.589%, Cl 0.164%-0.242%, Na 0.107%-0.19%), minor (Fe 328-548 mg/kg, Mn 16.9-48.3 mg/kg, Zn 26.8-47 mg/kg, Cr 1.41-13.8 mg/kg, Co 0.219-0.297 mg/kg, V 0.37-0.62 mg/kg), and non-essential elements (0.0325-393 mg/kg). Quality control was ensured using Zscore and Uscore statistical evaluation parameters, confirming data reliability and interval conformity. Comparisons with literature from Turkey, Morocco, Pakistan, and Algeria highlighted unique elemental compositions and potential health implications. These findings add significant value to medicinal plant research.

Key words: *elemental analysis, medicinal plants, irradiation, concentration.*

ملخص

تقدم هذه الدراسة تحليلاً مقارناً للعناصر الأساسية والسامة في نبات الغار (لوروس نوبيليس) والضرو (بيستاسيا لونتيسكوس) وإكليل الجبل (روزمارينوس اوفسيسناليس) باستخدام تقنية التحليل بالتنشيط النيوتروني k_0. قدمت هذه التقنية حساسية ودقة عالية في تحديد كميات العناصر. تشمل العناصر المكتشفة عناصر رئيسية (الكالسيوم ٠.٥٩-٠.٣٥٦، البوتاسيوم ٠.٦٧٣-٠.٧٤١، المغنيسيوم ٠.١٠٢-٠.٩٨٥، الكلور ٠.٤٦١-٠.٢٤٢، الصوديوم ٠.٧٠١-٠.٩١٠)بالمائة، وعناصر ثانوية (الحديد ٨٢٣-٨٤٥ ملغ\كغ، المنغنيز ٩.٦١-٣.٨٤ ملغ\كغ، الزنك ٨.٦٢-٧٤ ملغ\كغ، الكروم ١٤.١-٨.٣١ ملغ\كغ، الكوبالت ٠.٩١٢-٠.٧٩٢ ملغ\كغ، الفاناديوم ٠.٧٣-٠.٢٦ ملغ\كغ) وعناصر غير أساسية (٠.٥٢٣٠-٣٩٣ ملغ\كغ). تم ضمان مراقبة الجودة باستخدام معايير التقييم الإحصائية، مما أكد موثوقية البيانات وتوافق الفواصل الزمنية. أظهرت المقارنات مع الأدبيات من تركيا والمغرب وباكستان والجزائر تركيبات عنصرية فريدة وآثاراً صحية محتملة. تضيف هذه النتائج قيمة

كبيرة لأبحاث النباتات الطبية.
الكلمات المفتاحية: النباتات الطبية، التحليل العنصري، تحليل التنشيط النيوتروني، العناصرالتحليل العنصري، النباتات الطبية، الإشعاع، التركيز.

Résumé

Cette étude présente une analyse comparative des éléments essentiels et toxiques dans Laurus nobilis, Pistacia lentiscus et Rosmarinus officinalis en utilisant l'Analyse par Activation Neutronique k_0. Cette technique a offert une sensibilité et une précision élevées dans la quantification des éléments. Les éléments détectés incluent des éléments majeurs (Ca 0.95%-1.653%, K 0.376%-1.47%, Mg 0.201%-0.589%, Cl 0.164%-0.242%, Na 0.107%-0.19%), des éléments mineurs (Fe 328-548 mg/kg, Mn 16.9-48.3 mg/kg, Zn 26.8-47 mg/kg, Cr 1.41-13.8 mg/kg, Co 0.219-0.297 mg/kg, V 0.37-0.62 mg/kg) et des éléments non essentiels (0.0325-393 mg/kg). Le contrôle de la qualité a été assuré en utilisant les paramètres d'évaluation statistique Zscore et Uscore, confirmant la fiabilité des données et la conformité des intervalles. Les comparaisons avec la littérature provenant de la Turquie, du Maroc, du Pakistan et de l'Algérie ont mis en évidence des compositions élémentaires uniques et leurs implications potentielles pour la santé. Ces résultats apportent une valeur ajoutée significative à la recherche sur les plantes médicinales.
Mots clés :*analyse élémentaire, plantes médicinales, irradiation, concentration.*